Doctoral Dissertation

博士論文

Single-cell information analysis reveals small intracellular and large intercellular variations increase cellular information capacity

(1 細胞情報量解析による小さな細胞内変動と大きな細胞間変動を介した正確な細胞情報伝達の解明)

A Dissertation Submitted for the Degree of Doctor of Philosophy

December 2019

令和元年　12 月　博士 （理学）申請

Department of Biological Science, Graduate School of Science,

The University of Tokyo

東京大学大学院理学系研究科

生物科学専攻

Takumi Wada

和田　卓巳

Abstract

In biology, signaling pathways must reliably convert stimulation intensity into signaling activity in the presence of two sources of variability: Intracellular variation arising from within a cell (also referred to as intrinsic noise) and intercellular variation arising from cell-to-cell variability (also referred to as extrinsic noise). An example of intracellular variation is the stochastic fluctuation of a biochemical reaction; examples of intercellular variation, are the differences in gene expression and protein abundance among cells. In most models of biological systems, cell-to-cell variability causing different cellular responses between cells have thus far been considered “noise” that reduces the ability of the system to distinguish between different stimuli. Previous studies applying information theory to signaling pathways have examined the information transmission capacity at the cell-population level in which intercellular variation contributes to uncertainty and is noise, or at the single-cell level in which intercellular variation is absent (Summary Fig. 1). However, intercellular variation has the potential to enable individual cells to encode different information. Here, I hypothesized that some physiological systems, such as skeletal muscle, are better represented by a multiple-cell channel (Summary Fig. 1), which is a communication channel composed of a sum of single-cell channels and showed that intercellular variation increases information transmission of skeletal muscle with C2C12 differentiated myotubes, isolated single-fibers of mice skeletal muscle.

With intercellular variation, average dose-response of multiple-cells becomes graded, and I called this effect “response diversity effect” (Summary Fig. 2). I found that intercellular variation can serve as information rather than noise through response diversity effect, resulting more gradual dose-response of multiple-cell channel than that of a single-cell channel.

In both C2C12 myotubes and isolated single-fibers, the intracellular variation was small and intercellular variation was large, which means that each cell responds accurately and reproducibly to a particular stimulus, but their responses differ from each other. It means that not only each cell can control its response accurately, but also the accuracy of the response of

a tissue is enhanced by response diversity effect, in which incorporated intercellular variation as information not noise In addition, I quantified the information transmission of human facial muscle contraction during intraoperative neurophysiological monitoring and found that information transmission of muscle contraction is comparable to that of a multiple-cell channel. Thus, the data in this study indicated that intercellular variation can increase information capacity of tissues.

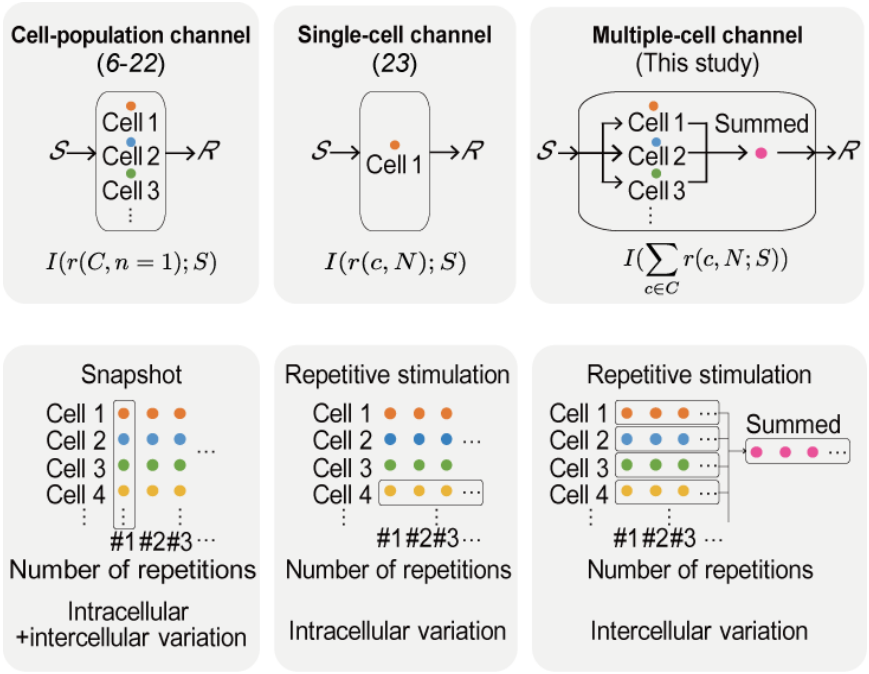

Summary Fig. 1. Schematic overview of cell-population, single-cell, and multiple-cell channel.

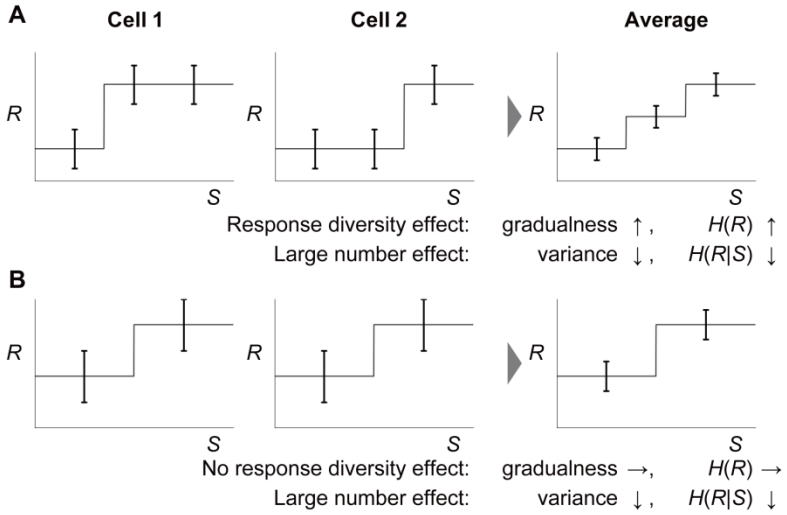

Summary Fig. 2. the effect on the dose-response of multiple-cell channel with (A) and without intercellular variation (B).

Table of Contents

1. Introduction

1.1 Intercellular and intracellular variation in signal transduction

In biology, signaling pathways transmit information about extracellular stimulation to control various cellular functions (*1*). These pathways must reliably convert stimulation intensity into signaling activity in the presence of two sources of variability: Intracellular variation arising from within a cell (also referred to as intrinsic noise) and intercellular variation arising from cell-to-cell variability (also referred to as extrinsic noise). An example of intracellular variation is the stochastic fluctuation of a biochemical reaction; examples of intercellular variation, are the differences in gene expression and protein abundance among cells (*2*, *3*). In most models of biological systems, cell-to-cell variability causing different cellular responses between cells have thus far been considered "noise" that reduces the ability of the system to distinguish between different stimuli. This limits how the dynamic range of a biological system is calculated and thus may not represent physiology.

1.2 Information analysis of signaling pathways in previous studies regarded intercellular variation as noise.

To determine the information transmission capacity of a relevant physiological system, skeletal muscle, I used mutual information (*4*, *5*), a mathematical principle for calculating the dependency between two variables (Fig. 1B). In most applications of mutual information, high variability reduces information transmission (Fig. 1A). Previous studies applying information theory to signaling pathways have examined the information transmission

capacity at the level of a population of cells (*6-22*) or of single cells (*23*) (Fig. 1C) (Table 1). These are referred to as channels, with the cell-population channel representing all of the cells as a single communication channel and the single-cell channel considering each cell individually. I hypothesized that some physiological systems, such as skeletal muscle, are better represented by a multiple-cell channel, which is a communication channel composed of a sum of single-cell channels (Fig. 1C). Unlike the cell-population channel in which intercellular variation contributes to uncertainty and is noise and the single-cell channel in which intercellular variation is absent, the multiple-cell channel incorporates intercellular variation as information (Fig. 1D). I propose that, by analyzing single-cell channels and incorporating these into a multiple-cell channel, I can accurately determine how much information is physiologically transmitted in a tissue or organ for which the response involves summing the output of the individual cells. Thus, I analyzed multiple-cell channels of Ca^{2+} response of C2C12 differentiated myotubes and the contraction of isolated single-fibers from flexor digitorum brevis (FDB) muscle of mice by electrical pulse stimulation (EPS) to investigate whether and how the intercellular variation increase information capacity of a skeletal muscle.

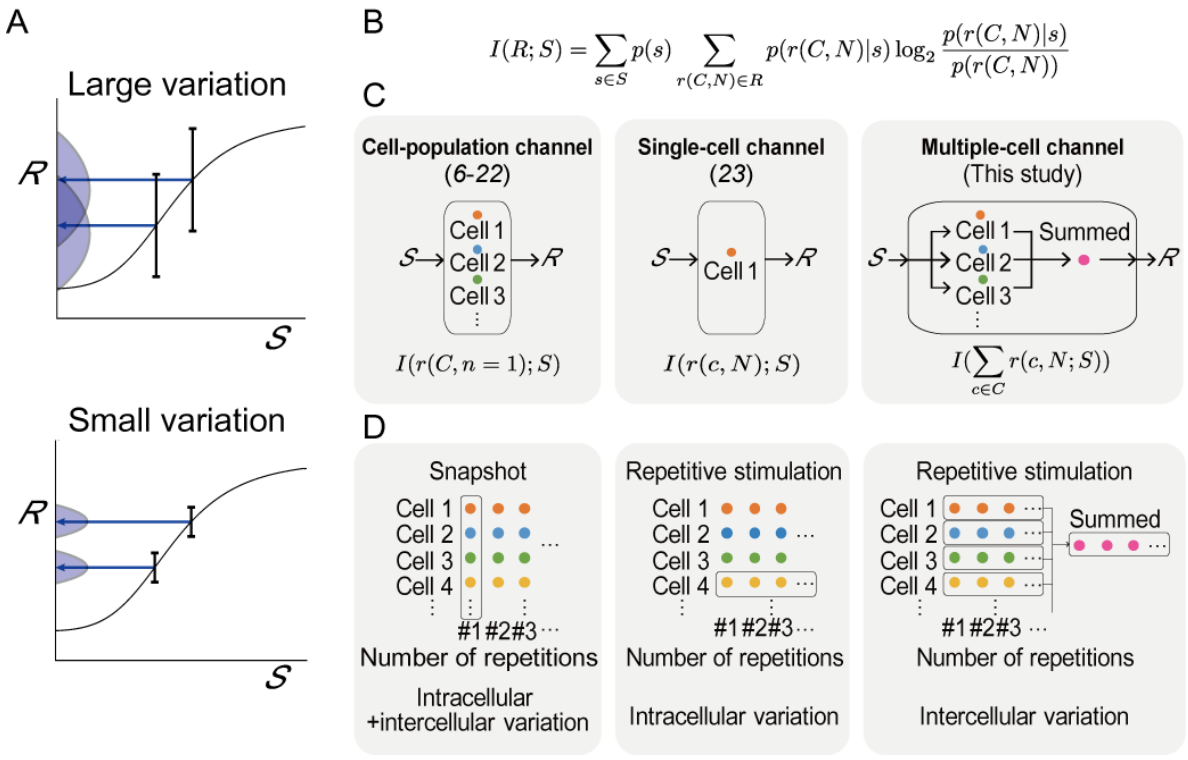

Fig. 1. Information transmission in a cell-population, a single-cell, and a multiple-cell channel. (**A**) The relationship between stimulation (*S*) and response (*R*) and the effect of variation on the ability to discriminate between high and low intensity stimulation. (**B**) Equation defining mutual information between stimulation and response. *S*, *R*, *C*, and *N* represent the set of stimulations, responses, cells, and the number of repetitions of stimulation, respectively. $p(s)$ and $p\big(r(C,N)\big)$ are probability distributions of stimulation intensity and response intensity, respectively, and $p(r(C,N)|S)$ is a conditional probability distribution of the response for a given stimulation. (**C and D**) Mutual information of a cell-population, a single-cell, and a multiple-cell channel. For a cell-population channel, response probability distribution is calculated from a single stimulation for each cell and includes both intracellular and intercellular variation as noise. For a single-cell channel, response probability distribution is calculated from repetitive stimulation for each cell and includes

intracellular variation as information. A multiple-cell channel, composed of a combination of single-cell channels, includes both intercellular and intracellular variation as information. Mutual information in the different channels differs in the definition of response *R*: For a cell-population channel, $R = r(C, n = 1)$; for a single-cell channel, $R = r(c, N)$; for a multiple-cell channe, $R = \sum_{c \in C} r(c, N)$, where $n \in N$ is the number of repetitions of stimulation and $c \in C$ is the cell.

Table 1. A summary of previous studies that calculated mutual information of signaling pathways. The mutual information calculated using cell-population channels, single-cell channels, and multiple-cell channels in previous studies and this study are summarized. Multiple-cell channel studies are indicated in bold. MI, mutual information.

Input	Output	MI (bits) (mean ± S.D.)	Channel	Sample Size per Dose	Literature
Bcd	Hb	1.5 ±0.15	Cell-population	< 1000	Tkačik *et al*. (*7*)
TNF	NF-κB, ATF-2	0.92, 0.85	Cell-population	350	Cheong *et al*. (*14*)
NGF, PACAP, PMA	pERK,pCREB, c-Fos,EGR1	> 1	Cell-population	1000～2000	Uda *et al*. (*16*)
EGF, ATP, LPS	ERK, Ca^{2+}, NF-κB	> 1.7	Cell-population	< 5320	Selimkhanov *et al*. (*18*)
GnRH	ppERK, EGR1, NFAT-NF, NFAT-RE	> 1	Cell-population	< 10000	Garner *et al*. (*19*)
ATP	Ca^{2+}	> 1.2	Cell-population	< 2500	Potter *et al*. (*20*)
Ach	Ca^{2+}	2.06 ± 0.31	Single-cell	5	Keshelava *et al*. (*23*)
EPS	Ca^{2+}	1.15 ± 0.52	Single-cell	20	**This study**
	Single-fiber Contraction	0.74± 0.29			
	Ca^{2+}	(512 cells) 3.21	**Multiple-cell**		
	Single-fiber Contraction	(512 cells) 2.65			
	Skeletal muscle contraction	(#1, Oris up) 2.83	**A tissue**	10	

1.3 Information transmission of skeletal muscle

The analysis of multiple-cell channel described above regarded the response of a tissue as the sum of the outputs of all individual cells in the tissue. However, a skeletal muscle *in vivo*, is innervated and controlled by multiple motor neurons with their own activation threshold. As the stimulation becomes stronger, the more muscle fibers are recruited (*24*). Thus, the contractile strength depends both on the contractile strength of the individual muscle fibers and on the number of the recruited muscle fibers. It is unclear whether the intercellular variation contributes to information capacity even in the presence of the effect of the recruitment. In order to solve this problem, I built the mathematical model considering the recruitment and calculated mutual information between EPS and the sum of Ca^{2+} response of a set of C2C12 myotubes recruited by the stimulation. I also calculated mutual information of human facial muscle contraction during intraoperative neurophysiological monitoring to quantify the information transmission in a skeletal muscle *in vivo*.

1.4 Purpose of this study

In summary, the purposes of this study are to analyze multiple-cell channels to clarify the contribution of the intercellular variation which was regarded as noise in previous studies. I investigated the contribution of intercellular variation to the increase in mutual information of multiple-cell channels and found that the intercellular variation enables the muscle systems to encode the high amount of information even in the presence of the effect of the recruitment.

2. Materials and Methods

2.1 Cell culture and the establishment of C2C12 cell lines stably expressing GCaMP

C2C12 cells (kindly provided by Takeaki Ozawa, University of Tokyo, Tokyo, Japan) were cultured in Dulbecco's Modified Eagle's Medium (DMEM; 25 mM glucose; Wako, Japan) supplemented with 10% fetal bovine serum (Nichirei Bioscience Incorporated, Japan) in an incubator at 37°C under a 5% CO2 atmosphere.

C2C12 cells stably expressing the Ca^{2+} biosensor, GCaMP6f (addgene #40755) (*25*), were established with the PiggyBac Transposase System (System Biosciences, U.S.A.) (*26*). One hundred and fifty μL of Opti-MEM (Life technologies, U.S.A.) containing 4 μL of Lipofectamin 2000 (Invitrogen, U.S.A.), and Opti-MEM containing 1.0 μg of PiggyBac transposon vector clone and 0.2 μg of PiggyBac transposase expression vector were mixed and incubated for 5 min. Thereafter, 50% confluent C2C12 cells were seeded on a 35-mm dish, transfected with the mixture, and incubated for 6 h. For the selection of transfected cells, the cells were cultured with DMEM with 10% fetal bovine serum and 20 μg/mL of Blasticidin S Hydrochloride (Wako, Japan). Selected cells were seeded on a Cell Culture Dish (Corning Incorporated, U.S.A.) and cultured until colonies formed. The colonies were picked and seeded on a Cell Culture Dish 430167. After seeding and proliferation, the cells were stored at a concentration of 1.0×10^5 cells/mL with Bambanker (NIPPON Genetics, Japan).

2.2 Differentiation induction of C2C12 cells

C2C12 cells were seeded into 4-well rectangular plates (Thermo Fisher Scientific, U.S.A.) at

a density of 2.0 x 10^5 cells/well, with 3 mL of 25 mM glucose DMEM supplemented with 10% fetal bovine serum. After 2 days, the medium was switched to a differentiation medium consisting of 25 mM glucose DMEM supplemented with 2% horse serum (Nichirei Bioscience Incorporated, Japan). Ten days after differentiation, cells were used for electrical pulse stimulation (EPS) (*27*).

2.3 Fluorescence Microscopy and Electrical pulse stimulation (EPS) to C2C12

Differentiated C2C12 myotubes stably expressing GCaMP6f were washed 3 times with PBS and starved in 3 mL fresh Medium 199, Hanks' Balanced Salts (Life technologies, U.S.A.) for 1 hour. Mineral oil (Sigma Aldrich, U.S.A.) was stratified to prevent vaporization of the medium prior to the fluorescence imaging. Fluorescence imaging was performed with an inverted fluorescence microscope, IX 83 (Olympus, Japan) equipped with a UPLSAPO10X2 objective lens (Olympus, Japan) an ORCA-R2 C10600-10B CCD camera (Hamamatsu Photonics, Japan), a U-HGLGPS mercury lamp (Molecular Devices, U.S.A.), a U-FBNA mirror unit (Olympus, Japan), an MD-XY30100T-META automatically programmable stage position (Molecular Devices, U.S.A.). EPS was performed according to the method of Manabe *et al.* (*30*). The 4-well plates were connected to the electrical stimulation apparatus, a 4-well C-Dish (Ion Optix Corp., Milton, MA, USA), and stimulated by electric pulses generated by an electrical pulse generator (Uchida Denshi, Hachioji, Japan). Under the microscope, C2C12 myotubes were stimulated with electric pulses of various voltages for 3 ms every 10 seconds. The exposure time was 25 ms for each image and 70 time-lapse images

for each of the 551 cells were acquired for each stimulation. Cells were repetitively stimulated for 20 times each of 10 different voltages, 0, 5, 10, 15, 20, 30, 40, 50, 60, 75 V. A single cycle was composed of one of each of the 10 voltages and each cycle was repeated 20 times, randomizing the order of stimulation independently every cycle. The timing of EPS was controlled with DIO-0808TY-USB digital I/O terminal (CONTEC, Japan) and EPS was imposed 400 ms after opening the shutter of the camera (Fig. 2).

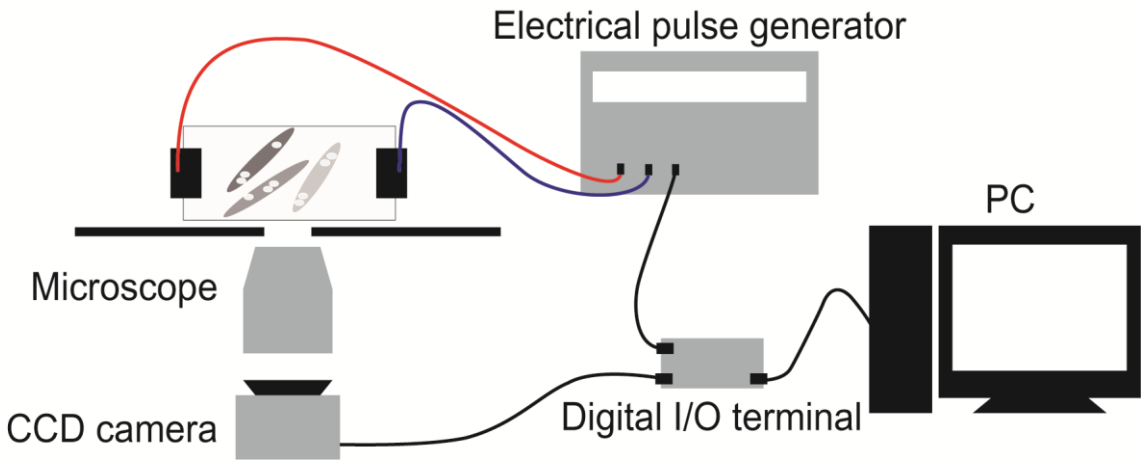

Fig. 2. Experimental setup of EPS-dependent Ca^{2+} response in C2C12 myotubes and of cell-contraction in single-fiber cells. When the signal reached the digital I/O terminal from the computer (PC), the terminal sent the signals to the CCD camera and the electrical pulse generator to start both image acquisition and EPS. For C2C12 myotubes, the terminal sent a signal to the camera 400 ms before the signal to the electrical pulse generator. For single-fiber cells, the terminal sent a signal to the camera 50 ms before the signal to the electrical pulse generator. Signal was then sent to the electrical pulse generator every one second.

2.4 Quantification of Ca^{2+} response

After background subtraction from Ca^{2+} time-lapse images acquired by fluorescent microscopy, regions of interest (ROIs) in C2C12 myotubes were selected manually. The time course data for the Ca^{2+} response of each C2C12 myotube were acquired by averaging intensity within each ROI for each image. Basal Ca^{2+} was defined by time average of 16 time points before any stimulation, and Ca^{2+} amplitude was defined by the maximum Ca^{2+} response subtracted by the basal Ca^{2+}. AUC was defined by the sum of the difference between Ca^{2+} response and the basal Ca^{2+}, multiplied by time step 25 ms.

2.5 Single-fiber isolation from a skeletal muscle

Satellite cells were prepared as described previously with modification (*28*). Briefly, 12 week-old C57/BL6J mice were sacrificed by cervical dislocation and the flexor digitorum brevis muscle (FDB) was gently removed. Dissected muscles were then digested in 0.25% collagenase solution (Collagenase Type1; Worthington, Lakewood, NJ) consisting of GlutaMAX Dulbecco's Modified Eagle's Medium (DMEM) supplemented with 1% penicillin-streptomycin and 10% fetal bovine serum (Corning, NY, USA) at 37 °C for 150 min. All tubes, dish, and pipets were coated with 5% bovine serum albumin (BSA) solution in PBS to avoid the adhesion of fibers. FDB was then transferred to a 50-mm Petri dish containing 8 mL of DMEM solution supplemented with 1% penicillin-streptomycin. Under a stereoscopic microscope, the muscles were gently disassembled using 1 mL pipettes to separate them into individual muscle fibers. Cell debris was completely removed by

exchanging the solution for fresh DMEM solution numerous times, and 50 fibers were transferred to a 1.5 mL centrifuge tube. The tubes were upright for 5 min to allow the fibers to settle to the bottom, the supernatant was gently aspirated using a Pasteur pipette, and 1 mL of fresh DMEM supplemented with 1% penicillin-streptomycin was added. All of the solution containing the fibers was transferred to 2-well Lab-Tek™ II Chamber Slide (Thermo Fisher Scientific, Waltham, USA) containing 1 mL of fresh DMEM supplemented with 1% penicillin-streptomycin.

2.6 Microscopy and EPS-dependent contraction of single muscle fibers

Individual fibers of FDB were stimulated with an electric pulse system developed previously for the C2C12 or primary myotubes contraction (*29*, *30*). The 2-well Chamber Slide was connected to the electrical stimulation apparatus and a 2-well electrode (Uchida-denshi, Hachioji, Japan), and fibers were stimulated with electric pulses generated by the power supply (Uchida-denshi). A stimulation cycle consisted of 3 ms duration of EPS and 997 ms intervals at 1 Hz for 10 sec. The initial voltage was 0 V, and the voltage was increased by 0.1 V from 1.5 V to 4.5 V. Contraction of the fibers was recorded under the microscope with the objective lens (X4).

2.7 Image analysis and quantification of contraction of single skeletal muscle fibers

After selecting the region with only a single fiber, images were smoothed with a Gaussian filter and the edge region was enhanced with a Sobel filter. The edge-enhanced images were

binarized by triangle method. Noises, like spots of binarized images, were removed by the opening filter, holes in fiber region were filled, and noise was removed by the opening filter. The selected regions were regarded as single-fiber regions and the time course data for contraction of each fiber were acquired for each image by quantifying the areas in the selected regions. Basal was defined by time average of last 10 time points of the time course data, and maximal contraction was defined by basal subtracted by minimal area of the time course.

2.8 Calculation of probability distribution

Using an adaptive partitioning method (*31*), I calculate probability distributions of Ca^{2+} amplitude and fiber contraction from the experimental data at the single-cell level obtained by repetitive stimulation. I calculated the conditional probability distribution of the response for a given stimulation of a single-cell channel with the single-cell data obtained by repetitive stimulation and that of a cell-population channel with the cell-population data obtained in the first stimulation. *S, C,* and *N* represent the set of stimulation, cell, and the number of stimulations, respectively, and the response *r* is the function of *C* and *N* and can be expressed as $r(C,N)$. The conditional probability distribution of the response for a given stimulation is $p(r(C,N)|S)$. When $c \in C$ is the cell variable and $n \in \mathrm{N}$ is the repeat number variable, the conditional probability distribution of a single-cell channel of cell *c* is $p(r(c,N)|S)$, and the conditional probability distribution of a cell-population channel calculated by a single stimulation is $p(r(C,n=1)|\,S)$. By applying the adaptive partitioning method for the

experimental data of a single cell, I calculated the probability distribution of $p(r(c,N)|\,S)$. For that of the cell population at a single stimulation, I calculated probability distribution of $p(r(C,n=1)|\,S)$.

2.9 Calculation of the mutual information and channel capacity

The mutual information between probability variables *S* and *R* is given by

$$I(R;S) = \sum_{s\in S} p(s) \sum_{r\in R} p(r|s) \log_2 \frac{p(r|s)}{p(r)}, \qquad \text{(Eq. 1)}$$

where *S* is the stimulation and *R* is the response, and $p(r|s)$ is $p(r(c,N)|\,S)$ or $p(r(C,n=1)|\,S)$ as calculated from experimental data. The calculation of the mutual information requires an input probability distribution $p(s)$. An input probability distribution cannot be definitively determined in a biological system; however, the optimal input probability distribution for the maximal mutual information, referred to as the channel capacity, in the channel is often used as an input probability distribution. The channel capacity can be estimated by Blahut-Arimoto algorithm (*32*, *33*). In this study, I defined the "mutual information" the mutual information estimated with the optimal input probability distribution for the summed response of the total cells, and I defined "channel capacity" as the mutual information estimated with the optimal input probability distribution for each channel.

2.10 Intracellular and intercellular variations

The total variation of each input condition can be divided into intracellular and intercellular

variations. Intracellular variation is the sum of the variance of the total cells and can be written as follows:

$$intracellular.variation(s) = \mathrm{E}[\mathrm{Var}[r(c,n)|c,s]|s]. \quad \text{(Eq. 2)}$$

Intercellular variation is the sum of squares of the difference between the average of each cell and the average of all and can be written as follows:

$$intercellular.variation(s) = \mathrm{Var}[\mathrm{E}[r(c,n)|c,s]|s]. \quad \text{(Eq. 3)}$$

The total variation was defined by the sum of the intracellular and intercellular variations, and the contributions of intracellular and intercellular variations to the total variation were calculated.

2.11 Estimation of the bias in the mutual information calculation caused by sample size, a number of stimulation events at a given dose

I estimated the bias in the calculation of the mutual information using a Hill equation response model (Fig. 5). The average dose-response was fixed and assumed that to obey the Hill equation,

$$r = \frac{s^n}{s^n + K_D^n}, \quad \text{(Eq. 4)}$$

where *s* is the stimulation variable, *r* is the response variable, *n* is the Hill coefficient and K_D is the dissociation constant. In the toy example shown in Fig. 5, K_D is 30 and *n* is 4. I examined the bias caused by small sample size (in the experiments in this study, the number of repetitions of the EPS at each voltage) by adding the Gaussian noise with various standard deviation. On this model, the response is expressed as follows:

$$r = \frac{s^n}{s^n + K_D^n} + \epsilon, p(\epsilon) = \frac{1}{\sqrt{2\pi\sigma^2}} e^{\left(-\frac{\epsilon^2}{2\sigma^2}\right)}, \quad \text{(Eq. 5)}$$

where *s* is the stimulation variable, *r* is the response variable, ϵ is Gaussian noise with a mean of 0 and the standard deviation is σ. Gaussian noise is assumed to be independent and have the same variance for all input. On the assumption of continuously and uniformly distributed input from 0 to 75, the averaged dose-response was numerically integrated with respect to input so that interdose variation of response was calculated to 0.143. When α is defined as the ratio of intradose variation and the total variation, α is written by the expression:

$$\alpha = \frac{intradose.variation}{intradose.variation + interdose.variation}. \quad \text{(Eq. 6)}$$

So, intradose.variation can be expressed as follows

$$intradose.variation = interdose.variation \frac{\alpha}{1-\alpha}. \quad \text{(Eq. 7)}$$

When α is 0.02, 0.04, 0.08, 0.16, 0.32, 0.64 and 0.9, intradose variation is 0.054, 0.077, 0.112, 0.165, 0.260, 0.504, 1.135, respectively. These intradose variations were used for the standard deviation of Gaussian noise of the Hill model. I sampled various sizes of cells (3, 5, 10, 20, 40, 80, 200, 400, 800, 1000 cells) 30 times for each sample size from the Hill model and estimated the mutual information. I assumed that sample size 1000 is sufficiently large and has ignorable bias. Thus, the calculation bias was defined by the difference between the average mutual information of sample size 20, the number of repetitive stimulations at each voltage that I used in the experiment, and that of sample size 1000.

To examine how many cells there were in the experimental data with α smaller than that used in the model, intradose and interdose variations, and α of each cell were calculated as

follows;

$$intradose.variation(c) = \mathrm{E}[\mathrm{Var}[r(c,n)|c,s]|c], \quad \text{(Eq. 8)}$$

$$interdose.variation(c) = \mathrm{Var}[\mathrm{E}[r(c,n)|c,s]|c]. \quad \text{(Eq. 9)}$$

2.12 Calculation of the mutual information of a multiple-cell channel

I calculated the mutual information of a multiple-cell channel by calculating the probability distribution of the summed responses of multiple cells as follows:

$$p(\textstyle\sum_{c\in C} y(c,N))|\, S). \quad \text{(Eq. 10)}$$

The optimal input probability distribution for the summed response of the total cells was used to calculate the mutual information of multiple-cell channels. For a 2-cell channel, I calculated the mutual information for all combinations of pairs of the single cells. When the responses of 2-cells were combined, I used all combinations of the responses to the same stimulation (Fig 10A and 11C).

To investigate the contribution of the intracellular and intercellular variations to the increase in the mutual information achieved by combining single-cell channels, I calculated the mutual information of a multiple-cell channel composed of the same cell $I_s(R;S)$ (Fig. 10B and 11D, red lines) and the mutual information of a multiple-cell channel composed of different cells $I_d(R;S)$ (Fig. 10B and 11D, blue line). To calculate $I_s(R;S)$, I virtually created the multiple-cell channel by resampling responses 1, 2, 4, 8, 16, 32, 64, 128, 256, 512 times repetitively to the same stimulation from the same cell, randomizing the order of responses every time. $I_s(R;S)$ was defined as the mutual information of the summed

response of the virtual multiple-cells and was calculated once for each cell for each resample size. I calculated $I_{\mathrm{d}}(R;S)$ by resampling 1, 2, 4, 8, 16, 32, 64, 128, 256, 512 cells for the Ca^{2+} amplitude in C2C12 myotubes, and 1, 2, 4, 8, 16, 32 cells for the contraction of single fibers with replacement from the total cells. $I_{\mathrm{d}}(R;S)$ was defined as the mutual information of the summed response of the resampled multiple cells and calculated 100 times for each resample size. The resampling was performed independently for each resample size. The order of responses was randomized every time the response was resampled.

Because there were only 50 cells for single fibers, I extrapolated the standard deviation to 1, 2, 4, 8, 16, 32, 64, 128, 256, 512 cells and calculated an extrapolated $I_{\mathrm{d}}(R;S)$ (Fig. 14D, green line). I assumed that the average of dose-response reaches equilibrium and does not change over 50 cells, and the standard deviation of the average response becomes smaller as the number of cells increases. The noise obeys Gaussian distribution and is independent for all input. When *n* is the number of cells, the average of *n*-cell summed response is

$$\mu(n) = \mu(50) * \frac{n}{50}, \qquad \text{(Eq. 11)}$$

and the standard deviation of *n*-cell summed response is

$$\sigma(n) = \sigma(50) * \sqrt{\frac{\mathrm{n}}{50}}. \qquad \text{(Eq. 12)}$$

Note that the extrapolation using Eqs. 11 and 12 holds if some cells did not make any response at the given stimulation.

2.13 The contribution of $\boldsymbol{\Delta H(R)}$ and $\boldsymbol{\Delta H(R|S)}$ to $\boldsymbol{\Delta I(R;S)}$

The mutual information can be expressed by the entropy of response $H(R)$, and the

conditional entropy of response for a given stimulation $H(R|S)$ as follows:

$$I(R;S) = H(R) - H(R|S). \quad \text{(Eq. 13)}$$

With the input probability distribution and the calculated response probability distribution, $H(R)$ and $H(R|S)$ can be calculated as follows:

$$H(R) = \sum_{s\in S} p(s) \sum_{r\in R} p(r|s) \log_2 p(r), \quad \text{(Eq. 14)}$$

$$H(R|S) = \sum_{s\in S} p(s) \sum_{r\in R} p(r|s) \log_2 p(r|s). \quad \text{(Eq. 15)}$$

The difference of the mutual information of two different channels, defined as $\Delta I(R;S)$, can be written as

$$\Delta I(R;S) = \Delta H(R) - \Delta H(R|S), \quad \text{(Eq. 16)}$$

where $\Delta H(R)$ is the difference of the entropy of response, and $\Delta H(R|S)$ is the difference of the conditional entropy of response for a given stimulation. The differences were defined by

$$\Delta H(R) = H_n(R) - H_1(R), \quad \text{(Eq. 17)}$$

$$\Delta H(R|S) = H_n(R|S) - H_1(R|S), \quad \text{(Eq. 18)}$$

where $H_n(R)$ and $H_n(R|S)$ represent the average of $H(R)$ and $H(R|S)$ of 100 resampled populations of *n*-cell channels (Fig. 10C, D, 14E, F, 12).

2.14 Binary channel with Gaussian noise

I built the binary response model, with a fixed threshold in each cell but different among individual cells (Fig. 12). The response of each cell can be written as

$$r(s) = \begin{cases} 1 + \epsilon \ (\text{if } s \geq threshold) \\ 0 \ + \epsilon \ (\text{if } s < threshold) \end{cases}, \quad \text{(Eq. 19)}$$

where *s* is the stimulation variable, *r* is the response variable, ϵ is Gaussian noise with a

standard deviation of 0.1. The threshold is fixed in each cell but different among individual cells and is continuously and uniformly distributed from 0 to 1 in the cell population. I assumed two kinds of input probability distribution: One is continuous uniform distribution from 0 to 1, and the other is discrete uniform distribution of 0, 0.1, 0.2, 0.3, 0.4, 0.5, 0.6, 0.7, 0.8, 0.9, 1.0. I resampled 1, 2, 4, 8, 16, 32, 64, 128, 256, 512 cells 100 times from this model and calculated the average of $I_{\mathrm{d}}(R;S)$ for each number of cells when continuous and discrete input probability distribution was given.

2.15 Ethics committee certification

I complied with Japan's Ethical Guidelines for Epidemiological Research, and the study as approved by the Institutional Review Board and the Ethics Committee of Tokyo University Hospital. (3530-(1)). Subjects were recruited by the related law.

2.16 Patients

This study included 5 consecutively enrolled patients with a newly diagnosed AN (vestibular schwannoma) or CPA (cerebellopontine angle) meningioma treated with retrosigmoid surgery at the University of Tokyo Hospital (Tokyo, Japan) from 2018 through 2019. All patients were 15 years of age or older. Informed consents were obtained during the pre-operative explanation.

2.17 Intraoperative facial muscle monitoring/Continuous Direct FREMAP Monitoring

Continuous Direct FREMAP (Facial nerve Root Exit zone–elicited compound Muscle Action

Potential) Monitoring was performed as previously described (*34, 35*). Briefly, monopolar needle electrodes were placed on the orbicularis oculi and orbicularis oris (up and down) muscles, under general anaesthesia before surgical operation with a reference electrode placed on the shoulder. Anesthesia was controlled by an anesthesiologist and except for use of a short-acting induction agent (rocuronium bromide up to 0.9 mg/ kg of body weight) for the initial 30 minutes, paralytic agents were strictly avoided throughout the operation. I used the "the Neuropack MEE1200 recording system" (Nihon Kohden, Tokyo, Japan) as a recording system. During tumor excision, the surgeon identified the facial nerve root at the brainstem (on the root exit zone of the facial nerve) and placed a specially designed hat-shaped monopolar electrode (Ad-Tech Medical Instrument Corporation), called the FREMAP electrode. continuous monitoring of evoked facial nerve EMGs were recorded. In this monitoring, the facial nerve was electrically stimulated at a frequency of 1 Hz, Stimulation conditions were as follows: 0.1 mA step by step within a stimulation intensity of 0.1-2.0 mA at a frequency of 1-3 Hz with 10 repetitive stimulations.

2.18 Motor unit model

I modeled skeletal muscle contraction by EPS to a motor nerve as the composition of three serial channels, the channel from *S* to *N*, *N* to *M*, the and *M* to *R*. *S* denotes EPS, *N* denotes the response of motor neurons, *M* denotes the contraction of muscle fibers, and *R* denotes the summed muscle contraction. For *S*, I used 10 voltages; 0, 5, 10, 15, 20, 30, 40, 50, 60, and 75 V; voltage conditions for C2C12 experiment.

In the channel from *S* to *N*, *N* remains zero below a threshold of *S*, θ, and monotonically increases above θ (Fig. 19). I set the number of thresholds as divisors of 10: 1, 2, 5, and 10. *N* is an effective voltage given to *M*. If a number of thresholds is one, θ_1 is 0 V and *N* monotonically increase, meaning that *N* is equal to *S*. If a number of thresholds is two, θ_1 is 0 V and θ_2 is at 30 V. This means that for N_2, N_2 is 5 V when *S* is 40 V, N_2 is 10 V when *S* is 50 V, *etc*. I set θ as 0, 10, 20, 40, and 60 V for five thresholds, and as 0, 5, 10, 15, 20, 30, 40, 50, 60, and 75 V for ten thresholds. Note that each neuron has a different threshold, and that a neuron in the model does not physiologically indicate a single neuron, but many neurons having the same threshold.

In the channel from *N* to *M*, I assumed that the neurons with the same threshold control the fixed set of skeletal muscle fibers. I set the number of skeletal muscle fibers controlled by each set of neurons with the same threshold as 64 in Fig. 18, 20, and 1, 2, 4, 8, 16, 32, and 64 in Fig. 21. Each set of neurons with the same threshold transmits the effective voltage *N* to the fibers controlled by these neurons, and the contraction of skeletal muscle fibers, *M* change according to *N*. I substituted the skeletal muscle fibers for C2C12 Ca^{2+} response data. I constructed the channels with or without intercellular variation. In the channel with intercellular variation, responses were resampled from different cells. In the channel without intercellular variation, I virtually created the set of skeletal muscle fibers without intercellular variation responses by resampling responses repetitively from the same cell, randomizing the order of responses every time.

In the channel from *M* to *R*, I assumed that the muscle contraction *R* is the sum of *M*, the

sum of all muscle fibers.

I calculated the mutual information between EPS *S* and muscle contraction *R* for the channel with intercellular variation, $I_{\mathrm{d}}(R;S)$, and without intercellular variation, $I_{\mathrm{s}}(R;S)$. I performed a two-way ANOVA with number of neuron and group (with/without intercellular variation) as the independent variables, and mutual information as the dependent variable for each number of muscle fibers at each neuronal threshold. The Bonferroni adjusted *p*-values ($n = 7$; the number of panels) between mutual information and group were calculated.

2.19 Data and materials

Data are available online at http://kurodalab.bs.s.u-tokyo.ac.jp/ja/publication/info/wada/ .

3. Results

3.1 Examination of Experimental condition for information analysis

Calculation of mutual information for single-cell channels and multiple-cell channels requires acquiring data for the single-cell response (*R*) to repetitive stimulation (*S*) with various intensities (Fig. 1C, middle). Therefore, I measured the Ca^{2+} response induced by repetitive EPS in differentiated C2C12 myotubes (*29*) (Fig. 3 and 4). Using C2C12 cell lines stably expressing GCaMP6f, a fluorescent Ca^{2+} probe (*25*) and differentiated into myotubes, I found that the Ca^{2+} response to a single EPS lasted ~1 second and was consistent for 200 repetitive stimulations (Fig. 3). Thus, I avoided the technical problem of time variation in the response by repetitively stimulating each myotube 20 times at 10 different voltages. This paradigm not only produced a time-invariant response but was also sufficient to avoid underestimation of mutual information (Fig. 4). I also determined that, although an overestimation bias was present, it was small enough to have little effect on the calculation of the mutual information from data acquired with 20 repetitive stimulations of 551 clonal C2C12 myotubes (Fig. 5).

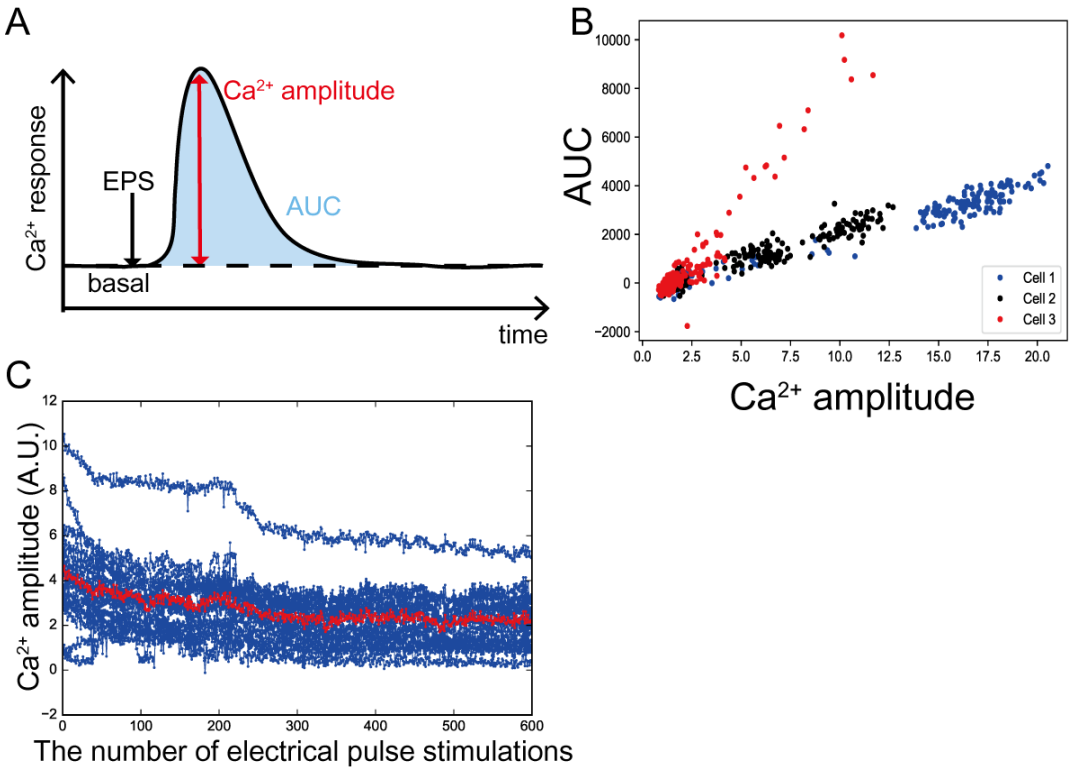

Fig. 3. The definition of Ca^{2+} amplitude and Ca^{2+} amplitude by repetitive EPS at 30V.

(**A**) Ca^{2+} amplitude (red arrow) and AUC (blue area) were defined (Materials and Methods). (**B**) Correlation coefficient between Ca^{2+} amplitude and AUC in each cell was 0.88 ± 0.13 (mean ± S.D.), indicating Ca^{2+} amplitude and AUC were positively correlated. I used Ca^{2+} amplitude as the feature value of Ca^{2+} response. (**C**) Ca^{2+} amplitude by repetitive EPS stimulation (30V). Blue: Ca^{2+} amplitude in each cell (*n*=19). Red: the ensemble average. The amplitudes of many cells remained the same through 200 stimulations. Amplitude decay started when the number of repetitions exceeded 200. I set the total number of repetitions to 200.

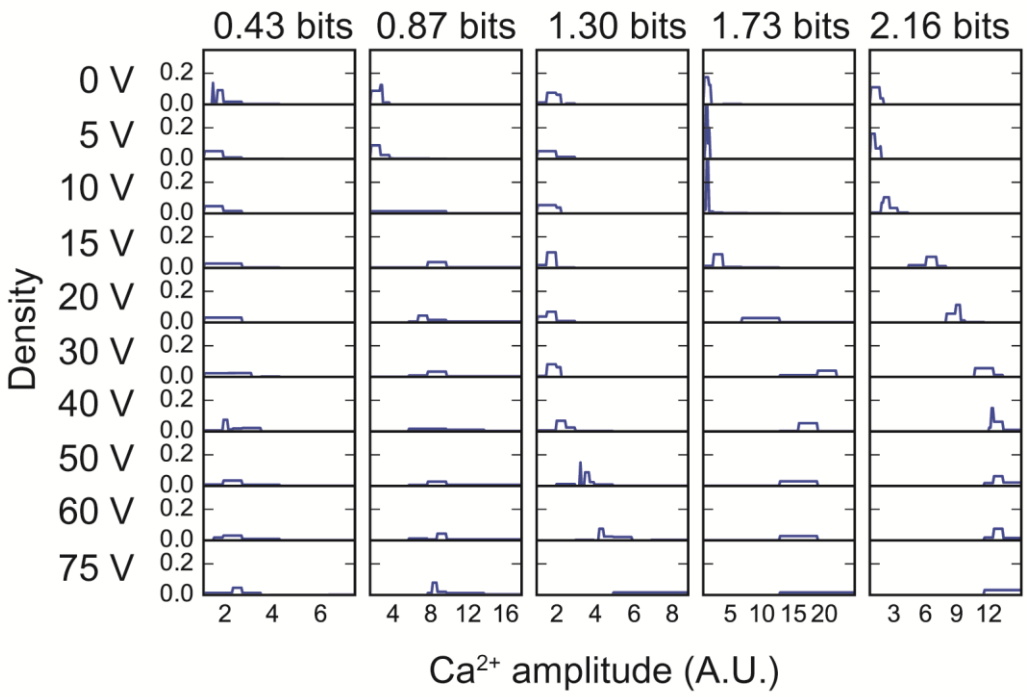

Fig. 4. The conditional probability distribution of Ca^{2+} amplitudes for a given stimulation of the cells having various mutual information. In setting the total number of stimulations, the number of inputs and the sample size in each stimulation has a trade-off relationship. Using the 10 conditions, 0, 5, 10, 15, 20, 30, 40, 50, 60, 75 V, I examined the conditional probability distribution of Ca^{2+} amplitude in C2C12 myotubes for a given stimulation. The mutual information for each myotube is indicated at the top and the data are presented in order of increasing mutual information. Because of few leaps of the position of probability distribution between adjacent input conditions for cells with various different mutual information, I concluded that these 10 conditions were sufficient to avoid underestimation of the mutual information in a single-cell channel.

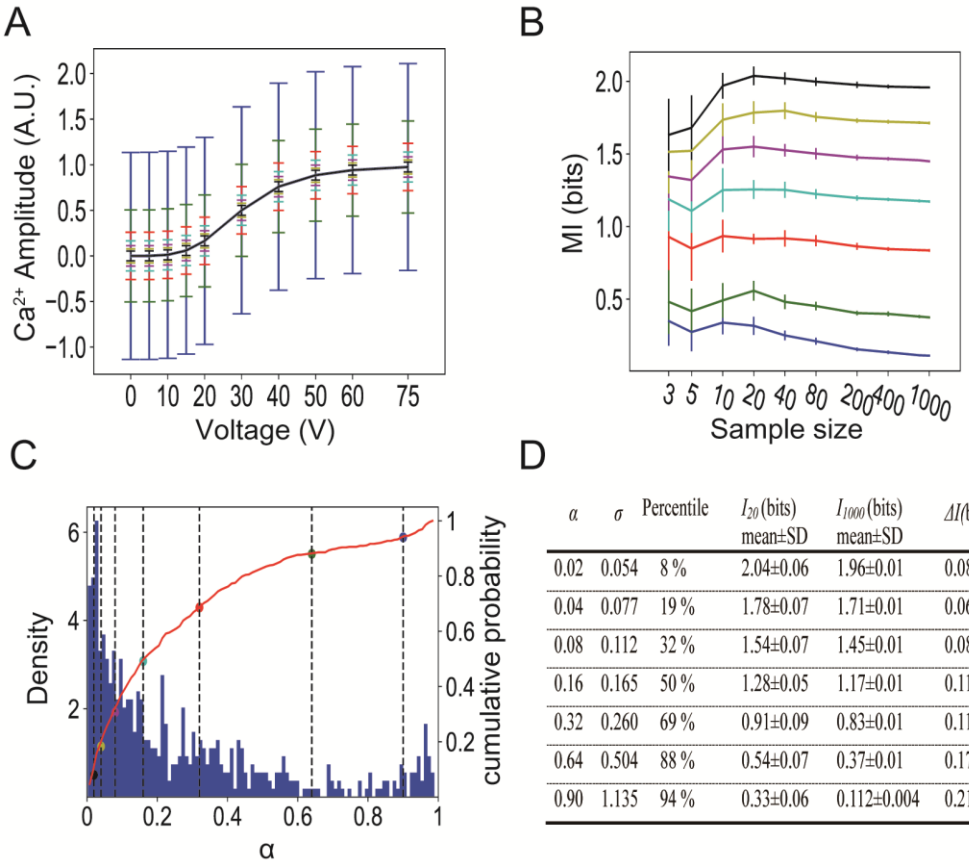

α	σ	Percentile	I_{20}(bits) mean±SD	I_{1000}(bits) mean±SD	ΔI(bits)	$2^{I_{20}} - 2^{I_{1000}}$
0.02	0.054	8 %	2.04±0.06	1.96±0.01	0.08	0.24
0.04	0.077	19 %	1.78±0.07	1.71±0.01	0.06	0.16
0.08	0.112	32 %	1.54±0.07	1.45±0.01	0.08	0.16
0.16	0.165	50 %	1.28±0.05	1.17±0.01	0.11	0.17
0.32	0.260	69 %	0.91±0.09	0.83±0.01	0.11	0.14
0.64	0.504	88 %	0.54±0.07	0.37±0.01	0.17	0.16
0.90	1.135	94 %	0.33±0.06	0.112±0.004	0.21	0.17

Fig. 5. Estimation of bias caused by sample size, the number of repetitions at each stimulation, calculated with a toy mathematical model. (**A**) A dose-response of the Hill model from a toy mathematical model of Ca^{2+} amplitude in response to 4 stimulations at each voltage. The model includes Gaussian noise with various standard deviations. In the Hill model, the response to the stimulation can be expressed as $r = \frac{s^n}{s^n + K_D^n} + \epsilon, p(\epsilon) = \frac{1}{\sqrt{2\pi\sigma^2}} e^{\left(-\frac{\epsilon^2}{2\sigma^2}\right)}$ (Eq. 5). In the example, K_D is 30, Hill coefficient n is 4, s is a stimulation variable, r is a response variable, ϵ is a Gaussian noise with a mean of 0, and the standard deviation is σ. α is defined as the ratio of intradose variation to the total variation, the sum of intradose and interdose variations (Eq. 6). When the values of α are 2, 4, 8, 16, 32, 64, and 90%, the values of intradose variation σ are 0.054, 0.077, 0.112, 0.165, 0.260, 0.504, and 1.135, respectively. Gaussian noise is added independently with each σ for all doses.

Color indicates noise at each α: 2% (black), 4% (yellow), 8% (magenta), 16% (cyan), 32% (red), 64% (green), and 90% (blue). (**B**) The relationship of sample size (number of repetitions of the stimulation) and calculated mutual information by adding Gaussian noises with various standard deviations. Bars indicate the standard deviation. (**C**) Histogram of calculated α of each cell from the experimental data (Eqs. 6, 8, and 9). Red line indicates the empirical distribution. Dashed line indicates the given α.

(**D**) The bias of mutual information when the sample size is 20. The value of α for the models is given, σ is the standard deviation calculated from the given α, "percentile" is the percentage of the cells with smaller α than the given value. As α becomes smaller, the smaller σ becomes. I_{20} and I_{1000} are the mutual information when sample sizes are 20 and 1000, respectively. $\Delta I = I_{20} - I_{1000}$ is the bias in the mutual information, and $2^{I_{20}} - 2^{I_{1000}}$ is the bias in the average number of controllable states. At a sample size of 20, representing the number of repetitive stimulations used in the experiments, bias in the number of controllable states was an overestimation ranging from 0.14 to 0.24. Because the data with the C2C12 myotubes resulted in 2.32 controllable states for a single-cell channel and 1.70 controllable states for a cell-population channel (determined from the optimal input), even the maximal bias (when α was 2%) does not affect the conclusion that a single-cell channel can transmit more information than a cell-population channel. Moreover, only ~8% of the myotubes had an α less than 2%. Therefore, I concluded that calculation bias existed but had little effect on results and interpretation and that the sample size of 20 repetitive stimulations at each voltage was adequate.

3.2 Information transmission of a single-cell channel in differentiated myotubes

From the analysis of 551 C2C12 myotubes, I observed that Ca^{2+} amplitude generally increased as the voltage increased (Fig. 6A); however, the dose-response of the Ca^{2+} amplitude varied from myotube to myotube (Fig. 6B). The variation of Ca^{2+} amplitude for each myotube was much smaller than that for the population (Total) (Fig. 6B, C). The larger variation of the population derived from large intercellular variation (Fig. 6D, Eqs. 2 and 3 in Materials and Methods). On average, intercellular variation accounted for 83% of the total variation, indicating that intercellular variation is much larger than intracellular variation for the C2C12 myotube Ca^{2+} response.

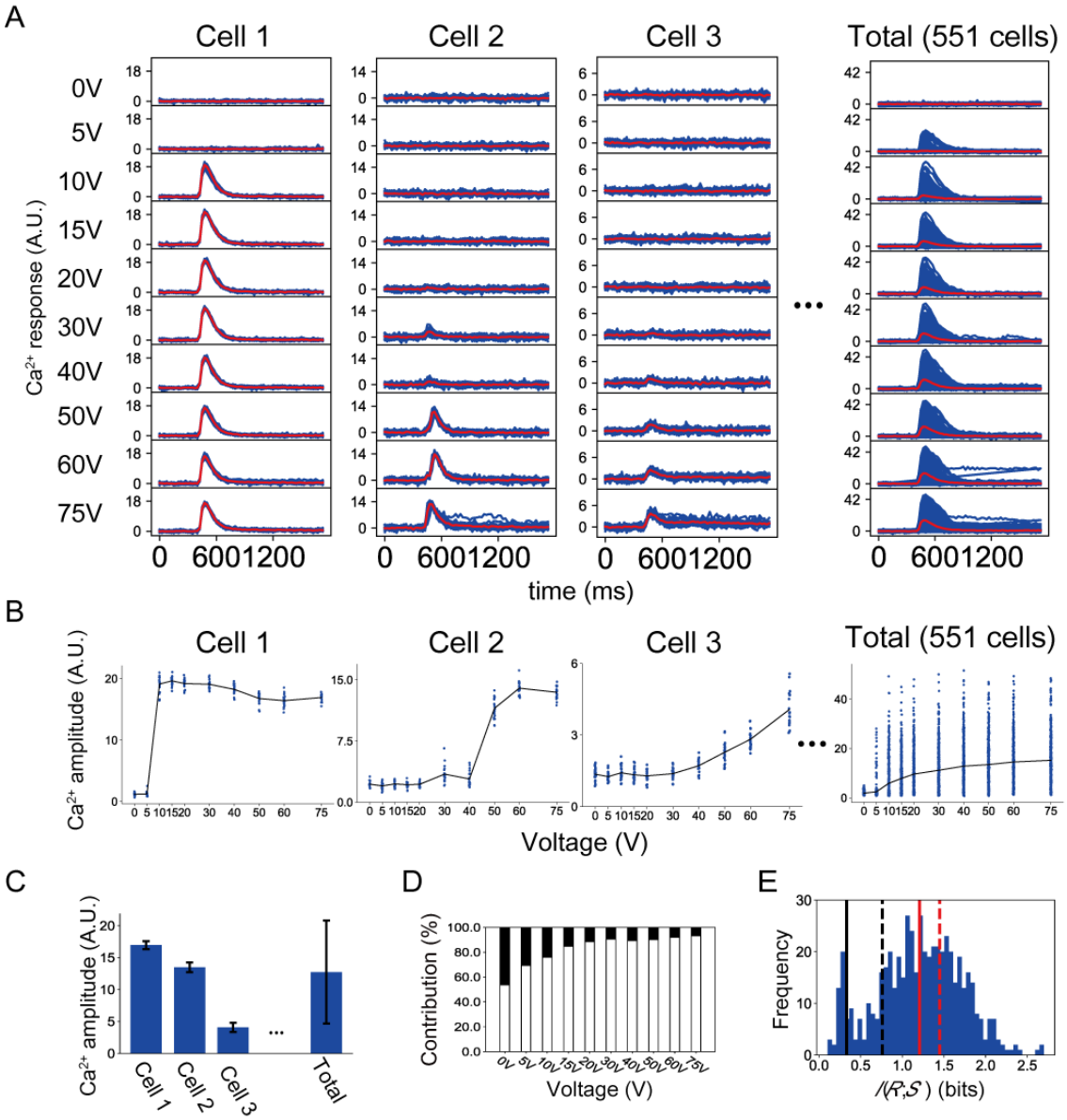
A
Cell 1
Cell 2
Cell 3
Total (551 cells)
0V
5V
10V
15V
20V
30V
40V
50V
60V
75V
Ca2+ response (A.U.)
time (ms)
B
Ca2+ amplitude (A.U.)
Voltage (V)
C
Ca2+ amplitude (A.U.)
Cell 1
Cell 2
Cell 3
Total
D
Contribution (%)
Voltage (V)
E
Frequency
I(R;S) (bits)

Fig. 6. Information transmission of a single-cell channel for electrical pulse stimulation into increases in Ca^{2+} amplitude in C2C12 myotubes. (**A**) Ca^{2+} response in individual differentiated C2C12 myotubes by repetitive stimulation (20 times) with 10 different intensities of electrical pulse stimulation (EPS). "Cell 1" to "Cell 3" are representative single-cell responses. "Total" indicates the responses in 551 myotubes. Each blue line indicates the Ca^{2+} response induced by single stimulation for each cell. Red lines indicate the summed response time course of the total cells. (**B**) Ca^{2+} amplitude versus voltage from the 3 cells shown in (A). A dot indicates Ca^{2+} amplitude to each single stimulation. Ca^{2+} amplitude is defined as the maximum response subtracted by basal Ca^{2+} before stimulation (Fig. 3). Black line, the average dose-response. (**C**) Average Ca^{2+} amplitudes induced by 75V EPS in individual C2C12 myotubes and in the total population. The error bars indicate standard deviations. (**D**) The percentages of intercellular (white) and intracellular (black) variation in the total variation for the indicated voltage of EPS (Eqs. 2 and 3 in Materials and Methods). (**E**) Histogram of the mutual information between intensity of EPS and Ca^{2+} amplitude in single-cell channels. Red dashed line, the average of channel capacity of a single-cell channel (1.45 bits); red solid line, the average mutual information of a single-cell channel (1.15 bits); black dashed line, channel capacity of the cell-population channel (0.76 bits); black solid line, the mutual information of the cell-population channel (0.33 bits). I used the optimal input probability distribution for the summed response of the total cells to calculate the mutual information (Fig. 7A, B), and the optimal input probability distribution for each channel to calculate channel capacity (see Materials and Methods).

To quantify how much information about voltage can be encoded in the amplitude of a Ca^{2+} response in a single-cell channel and cell-population channel, I calculated the probability distribution of Ca^{2+} amplitudes at each voltage for each myotube, calculated the mutual information of each single-cell channel relating voltage with Ca^{2+} amplitude, then plotted the frequency of the mutual information values for the 551 myotubes (Fig. 6E). I then calculated both the average mutual information and the channel capacity for the system represented as a single-cell channel and as a cell-population channel. I then calculated the average mutual information in a single-cell channel as 1.15 ± 0.52 bits (mean ± S.D.) (Fig. 6E, red solid line. See Materials and Methods, Fig. 7A, B for details). Each *n*-bit indicates 2^n states. The result indicates that among the 10 voltage conditions (10 states = $2^{3.32}$; that is 3.32 bits), on average a single-cell can distinguish 2.32 conditions (2.32 states = $2^{1.21}$). I calculated the mutual information in the cell-population channel as 0.33 bits (Fig. 6E, black solid line), indicating that on average the cell-population channel cannot distinguish between even 2 conditions. This means that as a population, the myotubes cannot distinguish even the presence or absence of stimulation. Thus, the single-cell channel transmitted more information than the cell-population channel, because the cell-population channel includes the high intercellular variation as source of uncertainty.

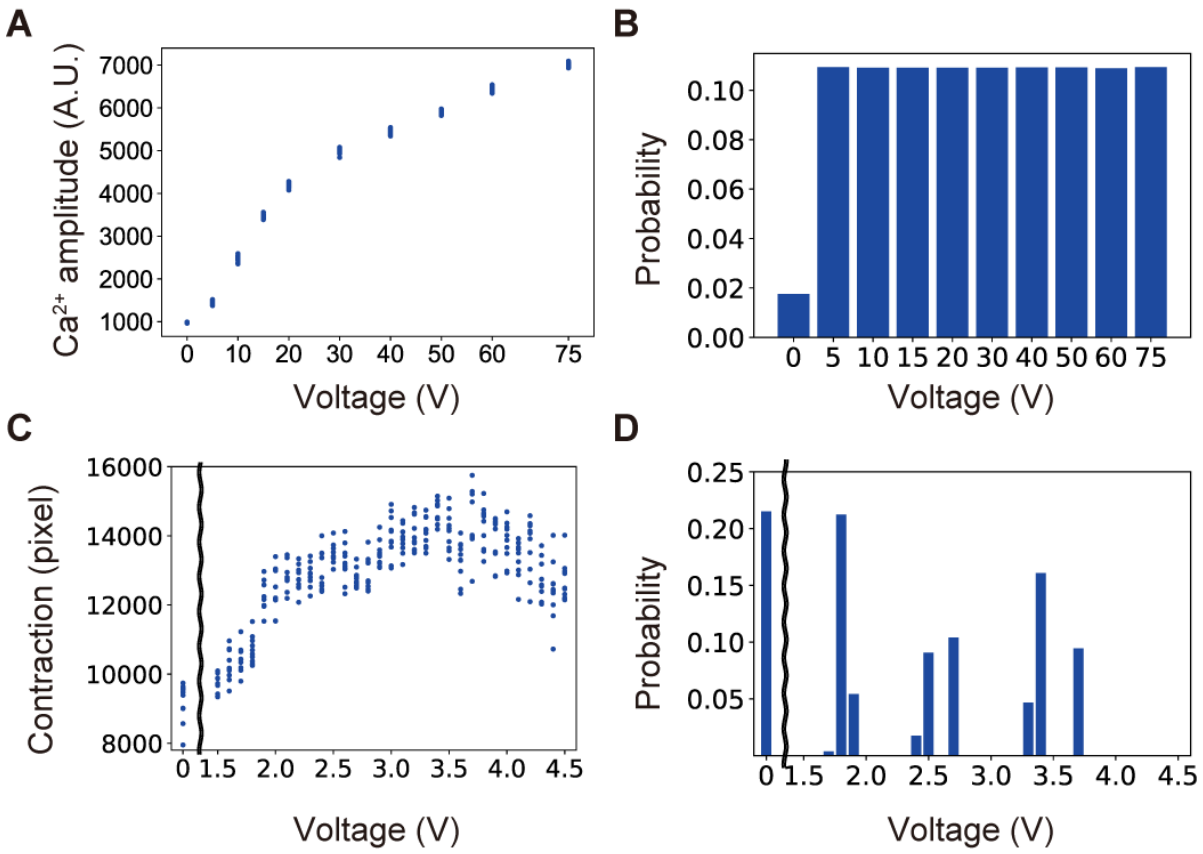

Fig. 7. The summed response of the total cells and the optimal input probability distribution for the summed response. (**A**) The summed response of the Ca^{2+} amplitudes at each voltage (0 – 75 V) for all 551 C2C12 myotubes. (**B**) The optimal input probability distribution for the summed response of the Ca^{2+} amplitude in all 551 C2C12 myotubes. (**C**) The summed response of contraction for all 50 skeletal muscle fibers stimulated from 0 – 4.5 V.(**D**) The optimal input probability distribution for the summed response of contraction of all 50 skeletal muscle fibers.

I calculated the channel capacity, which is the maximum amount of information that can be transmitted, of the single-cell channel as 1.45 bits on average (Fig 6E, red dashed line). Furthermore, there was a strong correlation (r = 0.947) between mutual information with the optimal input probability distribution for the summed response and channel capacity of single-cell channels (Fig. 8). Therefore, hereafter unless otherwise specified, I defined the "mutual information" as the mutual information calculated with the optimal input probability distribution for the summed response of the total cells, and I defined "channel capacity" as the mutual information calculated with the optimal input probability distribution for each channel. The channel capacity of the myotubes represented by a cell-population channel was 0.76 bits (Fig. 6E, black dashed line), which is similar to the 1-bit capacity found in previous studies of cell-population channels (Table 1) (*6*-*22*). I obtained similar results for the mutual information and channel capacities for single-cell channels and cell-population channels in two independent clones of C2C12 myotube lines stably expressing GCaMP6f (Fig. 9A, B). Additionally, these two clones also exhibited greater intercellular variation than intracellular variation (Fig. 9C, D).

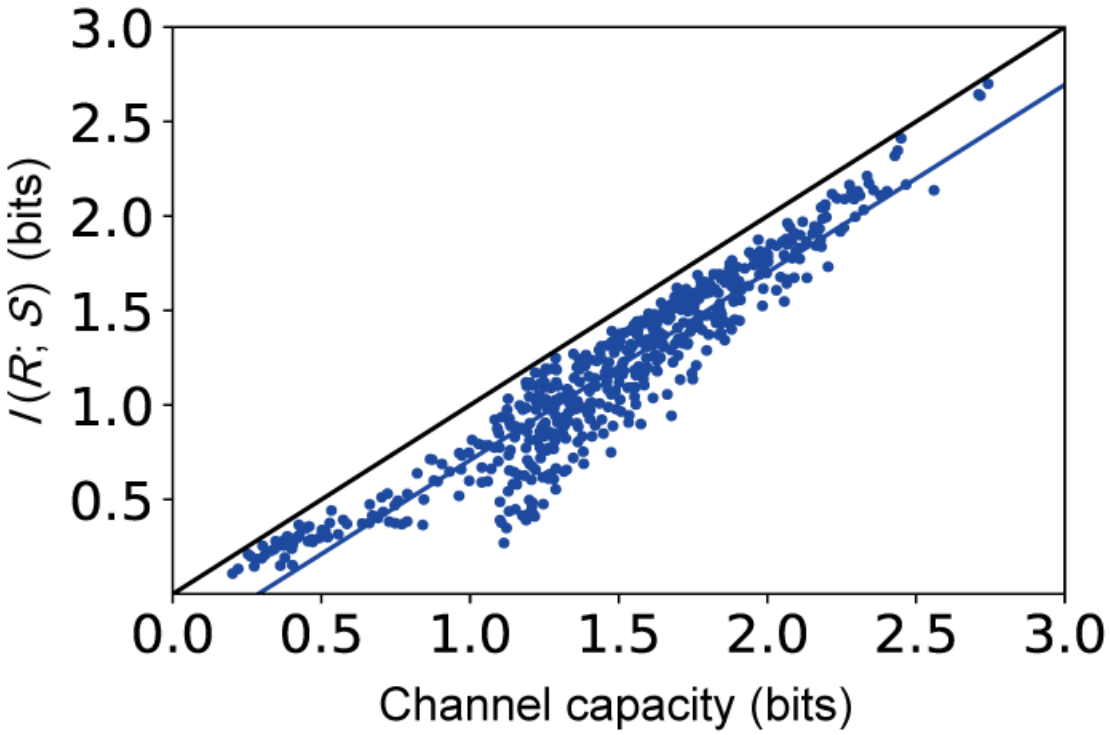

Fig. 8. Mutual information with the optimal input probability distribution for the summed response and channel capacity of single-cell channels in C2C12 myotubes. A dot indicates the mutual information calculated with the optimal input probability distribution for the summed response and the channel capacity of single-cell channels. The black line indicates $y = x$; the blue line indicates the regression line ($y = 0.993\,x - 0.285$ with correlation coefficient, 0.947). I used the optimal input probability distribution for the summed response of the total cells to calculate the mutual information, and I used the optimal input probability distribution for each single-cell channel to calculate the channel capacity.

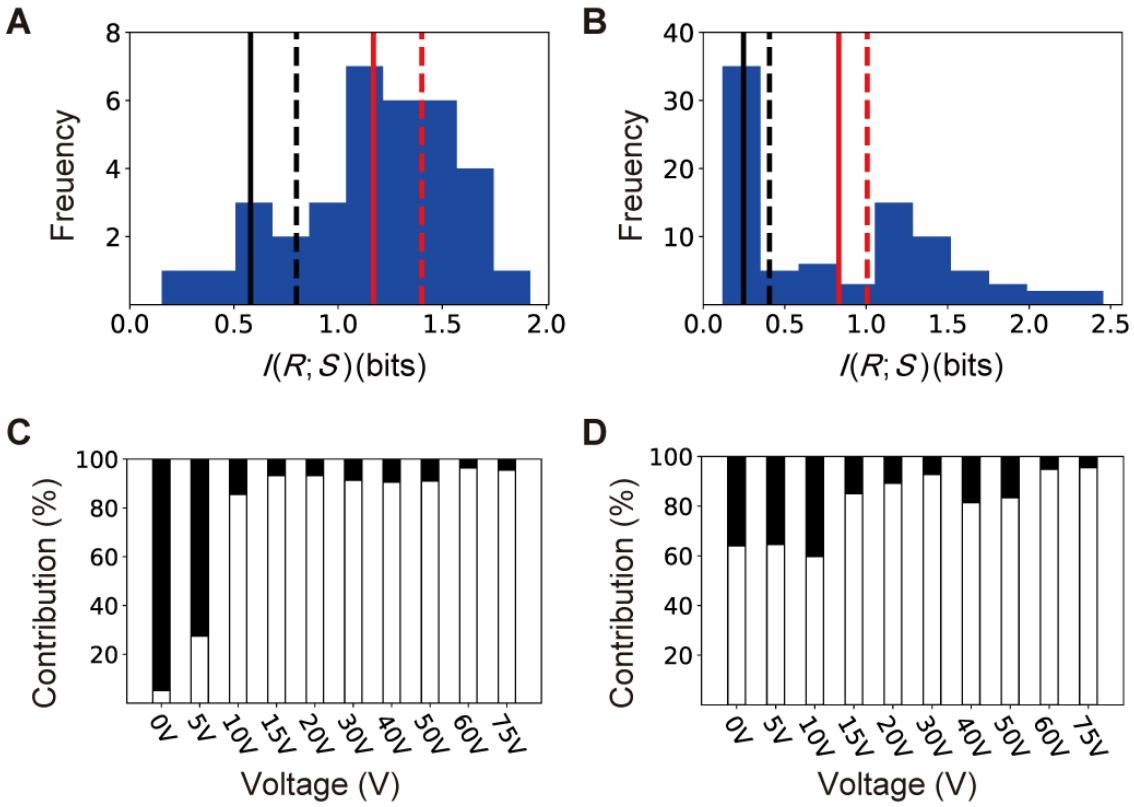

Fig. 9. Mutual information in two other independent clones (#2, #3) of C2C12 myotubes stably expressing GCaMP6f. (**A** and **B**) Histograms of mutual information of single-cell channels in clone #2 (A) and #3 (B). The numbers of cells of clone #2 and #3 were 34 and 86 respectively. Red solid line, the average of the mutual information of single-cell channels (1.19 bits for clone #2; 0.85 bits for clone #3); red dashed line, the channel capacities of single-cell channels (1.43 bits for clone #2; 1.02 bits for clone #3); black solid line, channel capacities of cell–population channels (0.75 bits for clone #2; 0.38 bits for clone #3); black dashed line, the mutual information of cell–population channels (0.55 bits for clone #2; 0.26 bits for clone #3 (B). In both clones, the average of the mutual information for single-cell channels was larger than that for a cell-population channel. (**C** and **D**) The percentages of intercellular (white) and intracellular (black) variations in the total variation by the indicated voltage of EPS in a clone #2 (C) and #3 (D) (Eqs. 2 and 3). In both clones, intercellular

variations were larger than intracellular variations. I used the optimal input probability distribution for the summed response of the total cells to calculate the mutual information, and I used the optimal input probability distribution for each channel to calculate the channel capacity (Fig. 9A, B, dashed lines).

3.3 Information transmission of a multiple-cell channel

In the cell-population channel, intercellular variation is regarded as uncertainty of signal intensity and represents noise. Therefore, the mutual information in the cell-population channel is lower than that in the single-cell channel. In contrast, by representing the single-cell channels as a multiple-cell channel, intercellular variation enables individual single-cells to encode different information, such as different signal intensities. Thus, I predicted that a multiple-cell channel composed of a sum of single-cell channels encodes more information than a single-cell channel (Fig. 10A). To examine this possibility, I calculated the mutual information of a 2-cell channel for every pair of myotubes (Fig. 10B). The 2-cell channel is a sum of two different single-cell channels (Eq. 10 in Materials and Methods). I summed the responses of two paired cells to calculate the probability distribution of the summed response, which I used as the response of a 2-cell channel to calculate the mutual information of a 2-cell channel. The average mutual information of the 2-cell channel was 1.55 ± 0.43 bits (mean ± S.D.) (Fig. 10B, black line). This result indicated that on average 2.94 conditions can be distinguished by a 2-cell channel. Thus, a 2-cell channel can transmit more information and distinguish more conditions than a single-cell channel, which only distinguished 2.32 conditions on average (Fig. 10B, red line). Moreover, increasing the number of cells in a multiple-cell channel increased the mutual information (Fig. 10C, blue). In the myotube experiments with 10 stimulation intensities, the mutual information plateaued with the inclusion of ~2^7 (=128) myotubes at 3.13 bits, because the mutual information approached the amount of information of input (3.32 bit). Consequently, the mutual

information for a multiple- cell channel with greater than 2^7 cells is likely underestimated.

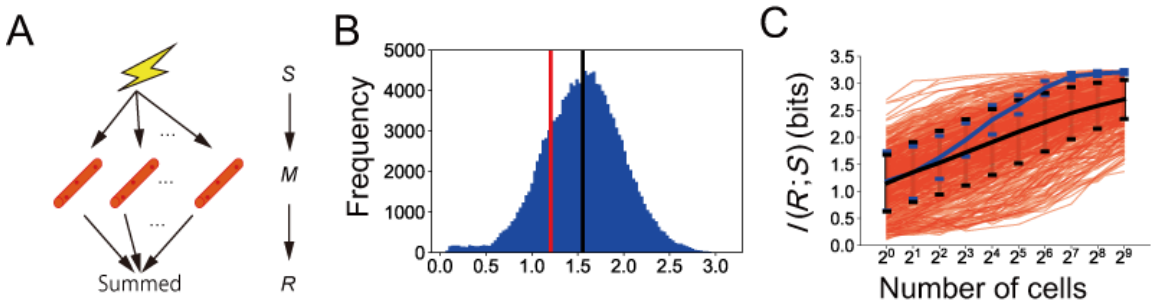

Fig. 10. Information transmission of a multiple-cell channel composed of single-cell channels. (**A**) A multiple-cell channel showing that the output of a multiple-cell channel is the sum of the output of single-cell channels. *S*, stimulus; *M*, multiple single cells; *R*, response. (**B**) Histogram of the mutual information of a multiple-cell channel comprised of 2-cell channels (Eq. 10 in Materials and Methods). Black line, the average mutual information of 2-cell channels (1.55 bits); red line, the average mutual information of single-cell channels (1.15 bits). (**C**) The mutual information of a multiple-cell channel according to the number of cells included as single-cell channels. Blue line, the average mutual information of a multiple-cell channel composed of single-cell channels from the 551 different myotubes, defined as $I_{\mathrm{d}}(R;S)$. Red lines, the mutual information of a multiple-cell channel composed of the same myotube by resampling responses repetitively from the same myotube, defined as $I_{\mathrm{s}}(R;S)$. Black line, the average of $I_{\mathrm{s}}(R;S)$. Bars indicate standard deviation for both black and blue lines.

3.4 Increase in information transmission by intercellular variation

To examine the contributions of intracellular and intercellular variations to the increase in the mutual information, I created a virtual multiple-cell channel composed of multiple instances of the same myotube. To generate this virtual channel, I resampled responses repetitively from the same cell, which eliminated intercellular variation. I then calculated the mutual information of a multiple-cell channel for each of the 551 myotubes (Fig. 10C, red). Hereafter, I define the mutual information of a multiple-cell channel composed of different myotubes as $I_{\mathrm{d}}(R;S)$ and that of the same myotube as $I_{\mathrm{s}}(R;S)$. For a 2-cell channel, about half of the myotubes had mutual information $I_{\mathrm{s}}(R;S)$ that was larger than the average $I_{\mathrm{d}}(R;S)$ (compare number of red lines with blue value at 2^1 on *x*-axis in Fig. 10B). However, as the number of myotubes in a multiple-cell channel increased, the average of $I_{\mathrm{d}}(R;S)$ (Fig. 10C, blue) gradually exceeded most of $I_{\mathrm{s}}(R;S)$ (Fig. 10C, red). Because $I_{\mathrm{d}}(R;S)$ includes intercellular variation and $I_{\mathrm{s}}(R;S)$ does not, intercellular variation appeared a key component for information encoding of a multiple-cell channel.

To understand how the mutual information of a multiple-cell channel exceeded that of a single-cell channel, I used another mathematical expression for the mutual information:

$$I(R;S) = H(R) - H(R|S).$$

$H(R)$ is the amount of information of the response; $H(R)$ is defined as the average logarithm of the number of distinguishable states of responses. $H(R|S)$ is the amount of information in the response for a given stimulation intensity; $H(R|S)$ is defined as the average logarithm of the number of response observed for a given stimulation intensity. The

mutual information becomes larger as $H(R)$ increases or $H(R|S)$ decreases. $H(R)$ can increase by averaging the different dose-responses of multiple-cells because the distinguishable number of responses increases. When different dose-responses, like those of Ca^{2+} increase of myotubes (Fig. 6B), are averaged, the dose-response relationship is graded (Fig. 11A, C). I called this effect "response diversity effect". On the other hand, $H(R|S)$ can decrease if the number of cells in the multiple-cell channel increases, because the variance in the averaged response decreases (Fig. 11A-C). I called this effect "large number effect". For a pair of identical cells, $H(R)$ cannot increase (Fig. 4B); thus, for $H(R)$ to change, there must be intercellular variation (Fig. 4A). For a pair of identical cells, the only way for the mutual information to increase is for the variance to decrease by testing the cell more times. I examined the contribution of a change in $H(R)$, $\Delta H(R)$ from the effect of intercellular variation and a change in $H(R|S)$, $\Delta H(R|S)$ to the increase in the mutual information of a multiple-cell channel with different myotubes or identical myotubes (Fig. 11D, E, Eqs. 14, 15, 17, and 18 in Materials and Methods). Both $\Delta H(R)$ and $-\Delta H(R|S)$ contributed to $\Delta I_{\mathrm{d}}(R;S)$ for the multiple-cell channel with different myotubes (Fig. 11D). Thus, both the response diversity effect and large number effect contributed to the increase in the mutual information of a multiple-cell channel composed of different myotubes. By contrast, only $-\Delta H(R|S)$ contributed to $\Delta I_{\mathrm{s}}(R;S)$ (Fig. 11E), indicating that only the large number effect contributed to the increase in the mutual information of a multiple-cell channel with the identical myotubes. The rate of the increase in $I_{\mathrm{d}}(R;S)$ as the number of myotube increased was larger than that of the increase in $I_{\mathrm{s}}(R;S)$ from 2^2 to 2^6 myotubes. This difference in the

rate of increase occurred in the different myotube model $\Delta H(R)$ increased. The decrease $\Delta H(R)$ that occurred for multiple-cell channels composed of more than 2^5 cells (Fig. 11D, E) is an artifact caused by underestimation of $\Delta H(R)$ from using discrete input probability distribution (Fig. 12). If the input probability distribution is continuous, $\Delta H(R)$ increases monotonically as the number of cells increases (Fig. 12). Thus, with a continuous input probability distribution, $\Delta H(R)$ would contribute to the increase in the mutual information for the entire range in multiple-cell channel with different myotubes. Intercellular variation causes the increase in $\Delta H(R)$; therefore, intercellular variation increases the information transmission of a multiple-cell channel.

A

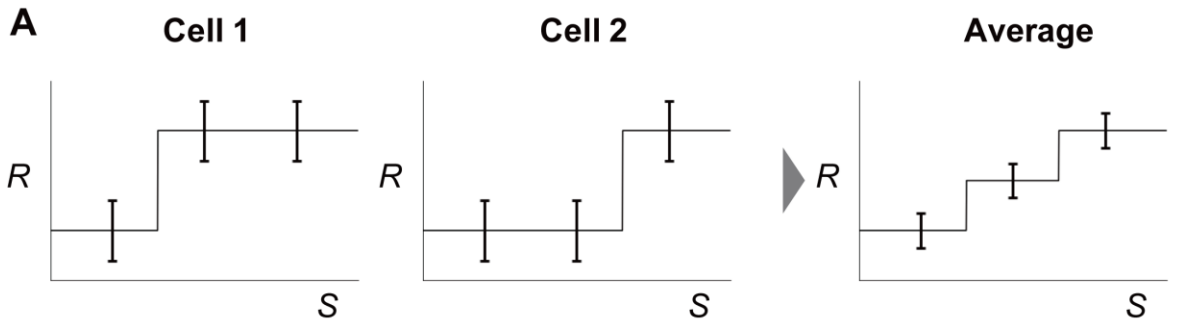

Response diversity effect: gradualness ↑, $H(R)$ ↑

Large number effect: variance ↓, $H(R|S)$ ↓

B

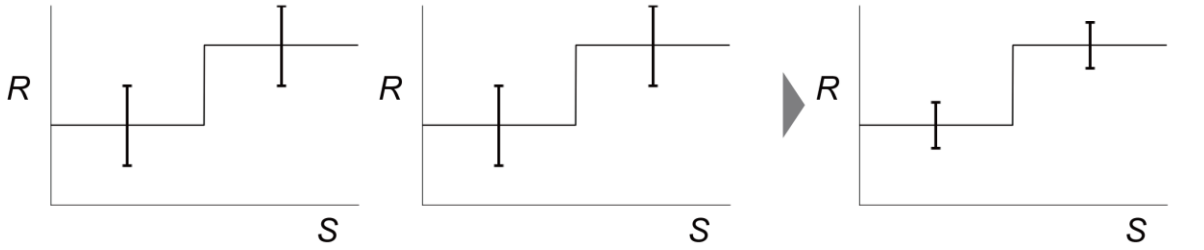

No response diversity effect: gradualness →, $H(R)$ →

Large number effect: variance ↓, $H(R|S)$ ↓

C

	Intercellular variation	Increase in a number of cells
Effect	Response diversity effect	Large number effect
Entropy change	Increase in $H(R)$	Decrease in $H(R\|S)$
Dose-response curve	Increase in gradualness	Decrease in variance

D

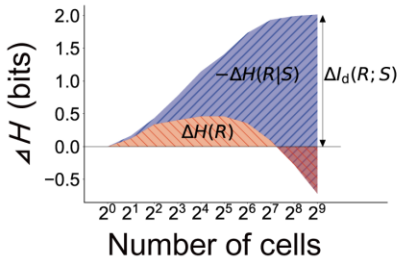

E

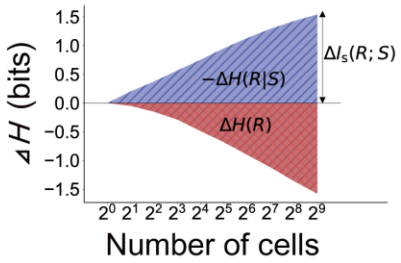

Fig. 11. The response diversity effect and the large number effect of 2 cells with different or identical responses on the mutual information of a 2-cell channel. (**A**) The effect of averaging a pair of cells with different dose-response relationships. (**B**) The effect of averaging a pair of cells with identical dose-response relationships. (**C**) The effects caused by intercellular variation and increase in a number of cells. (**D**) The contribution of the difference in the average $H(R)$, $\Delta H(R)$, and the difference in the average $-H(R|S)$, $-\Delta H(R|S)$, to differences in the average $I_{\mathrm{d}}(R;S)$, $\Delta I_{\mathrm{d}}(R;S)$, in a multiple-cell channel composed of different single-cell channels in the C2C12 Ca^{2+} response. The differences were defined by those between $H(R)$, $-H(R|S)$, $I_{\mathrm{d}}(R;S)$ for each number of cells and those whose size is 1 (Eqs. 16, 17, and 18 in Materials and Methods). (**E**) The contribution of $\Delta H(R)$ and $-\Delta H(R|S)$ to $\Delta I_{\mathrm{s}}(R;S)$ in a multiple-cell channel composed of the same single-cell channel. I used the optimal input probability distribution for the summed response of the total cells to calculate the mutual information.

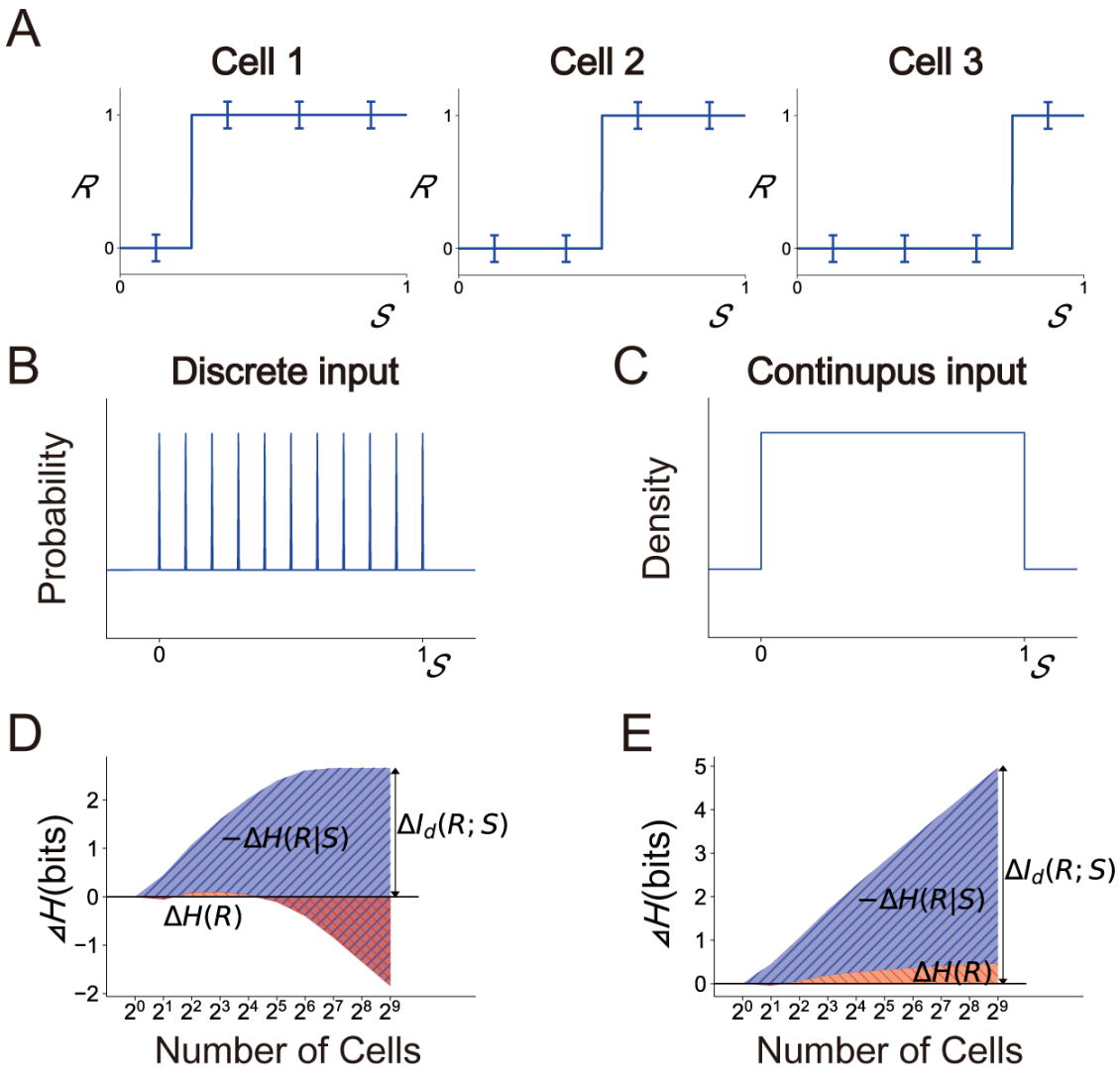

Fig. 12. The effect of discrete and continuous input on $\Delta H(R)$ and $-\Delta H(R|S)$ in a binary response model. (**A**) A binary response model, with a threshold that is different among individual cells and evenly distributed from 0 to 1 (Eq. 19) (Materials and Methods). Each cell responds 0 if *s* is smaller than the threshold and responds 1 if *s* is larger than the threshold. Gaussian noise with a standard deviation of 0.1 was added independently to the total cells and to the stimulation. (**B**) Discrete uniform input probability distribution of 0, 0.1, 0.2, 0.3, 0.4, 0.5, 0.6, 0.7, 0.8, 0.9, 1.0. (**C**) Continuous uniform input probability distribution from 0 to 1. (**D**) The contribution of $\Delta H(R)$ and $-\Delta H(R|S)$ to the mutual information in a multiple-cell channel composed of different single-cell channels, $\Delta I_{\mathrm{d}}(R;S)$, with discrete

input probability distribution. As the number of cells increases, $\Delta H(R)$ increases and then decreases. The differences $\Delta I_{\mathrm{d}}(R;S)$, $\Delta H(R)$, and $\Delta H(R|S)$ for each number of cells were defined by the differences from those when the number of cells is 1 (Eqs. 16, 17, and 18). (**E**) The contribution of $\Delta H(R)$ and $-\Delta H(R|S)$ to the mutual information in a multiple-cell channel composed of different single-cell channels, $\Delta I_{\mathrm{d}}(R;S)$, with continuous input probability distribution. As the number of cells increases, $\Delta H(R)$ increases monotonically. The differences $\Delta I_{\mathrm{d}}(R;S)$, $\Delta H(R)$, and $\Delta H(R|S)$ for each number of cells were defined by the differences from those when the number of cells is 1 (Eqs. 16, 17, and 18).

3.5 Information transmission in isolated skeletal muscle fibers

The Ca^{2+} response triggers skeletal muscle contraction, representing a final biological output. To evaluate information transmission in skeletal muscle contraction, isolated single fibers from FDB muscle of mice were isolated and electrically stimulated to induce contraction as a physiological output (*28*) by the collaboration with Tokyo Metropolitan University (see Acknowledgements). Contractions in response to 10 repetitive stimulations at 32 different voltages were measured and I calculated the mutual information between EPS and contraction (Fig. 13, 14) (Materials and Methods). Similar to the C2C12 myotube Ca^{2+} response, for the same voltage, contraction varied from fiber to fiber (Fig. 13). The variation of contraction for each fiber was much smaller than that across the population (Fig. 13B). The larger variation of the fiber population derived from a large intercellular variation (Fig. 14A, Eqs. 2 and 3 in Materials and Methods). Similar to the C2C12 myotubes, on average, intercellular variation accounted for 86% of the total variation.

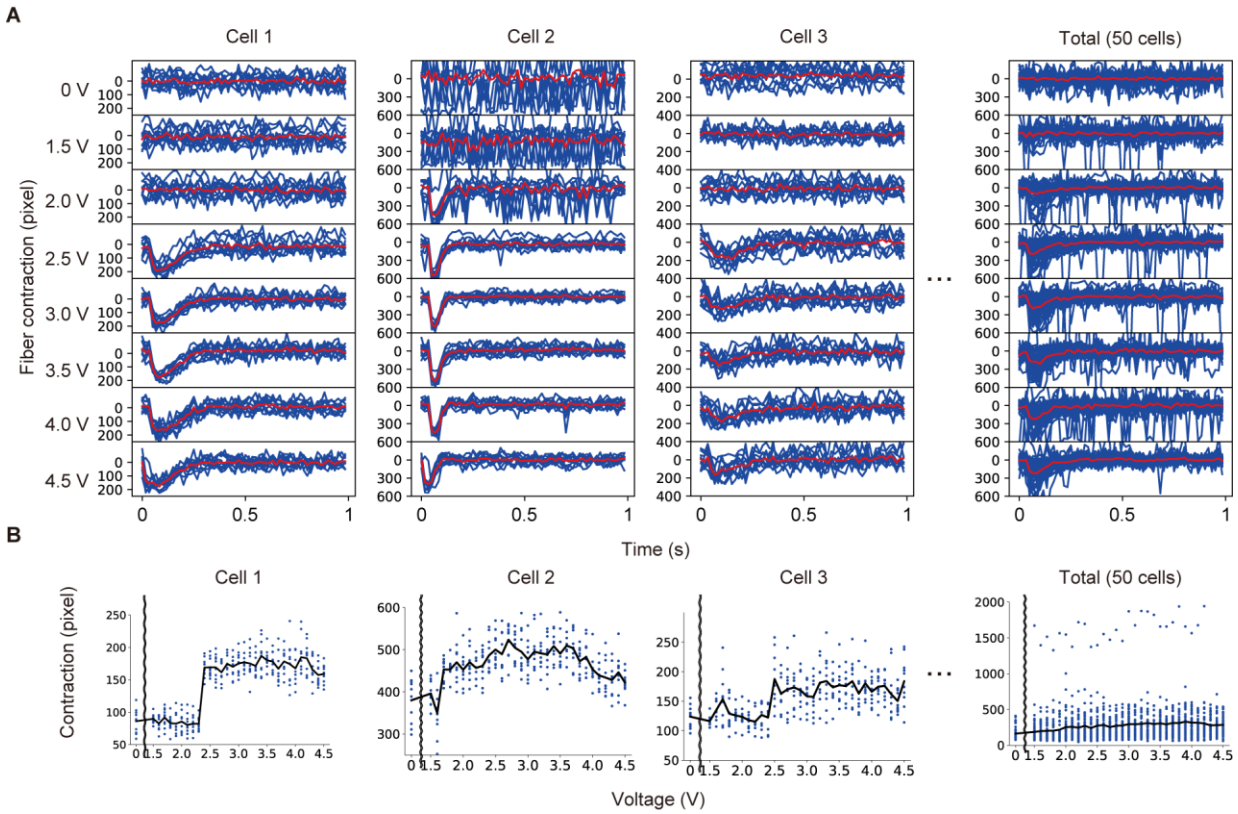

Fig. 13. Contraction of single muscle fibers. (**A**) Contraction in individual fibers in response to 10 times-repetitive stimulation with 32 different voltages of EPS from 0 – 4.5 V. "Cell 1" to "Cell 3" are representative of the contraction of single fibers. "Total" indicates responses in 50 fibers. Each blue line indicates a time course of the contraction by a single stimulation for each cell. Red lines indicate the averaged time course. (**B**) Dose-responses of contraction for the data shown in (A). A dot indicates maximal contraction induced by each single stimulation. Black line, the average dose-response.

As I did for the C2C12 myotubes, I calculated the summed response of all of the fibers (a total of 50) and calculated the optimal input probability distribution of the summed response of the total cells and used this to determine channel capacity (Fig. 7C, D). The experimental conditions and outputs are different, thus, the values for the mutual information for EPS-induced contraction of single-fiber cells and those for EPS-induced Ca^{2+} amplitude in C2C12 myotubes are not directly comparable. I calculated the mutual information between EPS and contraction in a single-cell channel for each cell (Fig. 14B) as 0.74 ± 0.29 bits (mean ± S.D.) (Fig. 14B, red solid line). I also calculated the mutual information in the cell-population channel and found that the mutual information of the cell-population channel was 0.25 bits (Fig. 14B, black solid line). Thus, similar to the mutual information for EPS-induced C2C12 myotube Ca^{2+} response, the mutual information for EPS-induced fiber contraction is greater when evaluated as a single-cell channel than as a cell-population.

Using the optimal input probability distribution for the summed response of the total fibers, I calculated the mutual information of 2-cell channels for each pair of fibers. The average mutual information of the 2-cell channel was 1.01 ± 0.32 bits (mean ± S.D.) (Fig. 14C, black, Eq. 10 in Materials and Methods), indicating that on average 2.02 conditions can be distinguished by a pair of fibers. Additionally, a 2-cell channel can transmit more information (2.02 conditions) than a single-cell channel for which only 1.67 conditions can be distinguished on average. As the number of the fibers composing the multiple-cell channel increased, the mutual information of the multiple-cell channel increased (Fig. 14D, blue), consistent with the increased information transmission that I observed by increasing the

number of the cells in the multiple-cell channel for the C2C12 myotubes. Using the same method that I used for the C2C12 myotube data (Fig. 10C), I generated $I_s(R;S)$ for 50 fibers (Fig. 14D, red lines). For a 2-cell channel, about 40% of $I_s(R;S)$ was larger than the average of $I_d(R;S)$. However, unlike the C2C12 myotube multiple-cell channel, when the number of cells in a multiple-cell channel increased, the percent of $I_s(R;S)$ (Fig. 14D, red) that exceeded the average $I_d(R;S)$ (Fig. 14D, blue) did not become smaller. However, at 50, the sample size of the single fibers is smaller than the 551 of C2C12 myotubes, thus I cannot conclude that $I_d(R;S)$ would not become larger than $I_s(R;S)$ if calculated for a larger number of cells. Therefore, I extrapolated the standard deviation of an *n*-cell summed response to larger numbers of cells and calculated $I_d(R;S)$ using this *n*-cell response (Fig. 14D, green, Eqs. 11, and 12 in Materials and Methods). This *n*-cell calculation showed the expected reduction in the percent of $I_s(R;S)$ (Fig. 14D, red) that exceeded the average of the extrapolated $I_d(R;S)$ (Fig. 14D, green). Thus, the muscle fiber system also transmitted more information as the number of cells of the multiple-cell channel increased as a result of the incorporation of intercellular variation.

I examined the contribution of $\Delta H(R)$ and $-\Delta H(R|S)$ to the increase in mutual information of a multiple-cell channel (Fig. 14E, F, Eqs 14, 15, 17 and 18 in Materials and Methods). The results were the same as for the C2C12 myotube system: Both $\Delta H(R)$ and $-\Delta H(R|S)$ contributed to the extrapolated $\Delta I_d(R;S)$ (Fig. 14E), whereas only $-\Delta H(R|S)$ contributed to $\Delta I_s(R;S)$ (Fig. 14F). Thus, for both fiber contraction and the Ca^{2+} response in C2C12 myotubes, both the large number effect and the response diversity effect increased

information transmission of a multiple-cell channel.

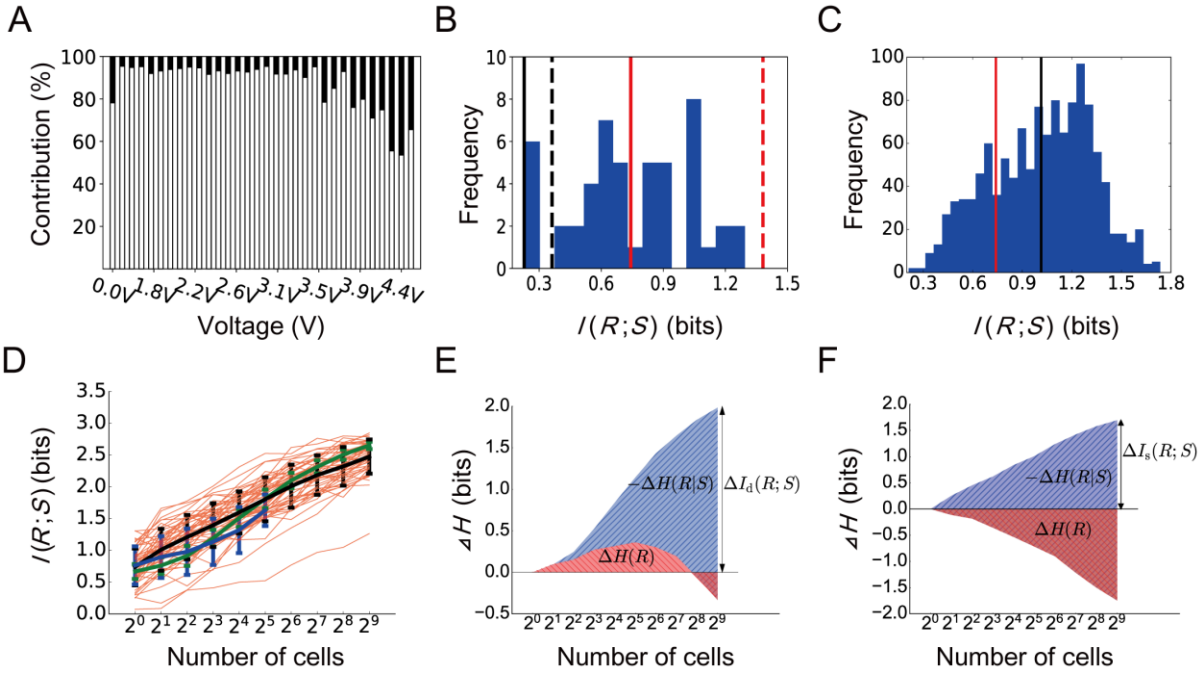

Fig. 14. Information transmission of a single-cell channel and a multiple-cell channel for electrical pulse stimulation into contraction of single skeletal muscle fibers. (**A**) The percentages of intercellular (white) and intracellular (black) variation in the total variation for the indicated voltage of EPS in single fibers (Eqs. 2 and 3 in Materials and Methods). The average intracellular variation was 86% of the total variation across all voltages. (**B**) Distribution of the mutual information between intensity of EPS and contraction in single-cell channels. Red dashed line, the average channel capacity of a single-cell channel (1.38 bits); red solid line, the average mutual information of a single-cell channel (0.74 bits); black dashed line, channel capacity of a cell-population channel (0.36 bits); black solid line, mutual information of a cell-population channel (0.25 bits). (**C**) Histogram of the mutual information of multiple-cell channel comprised of 2-cell channels (Eq. 10 in Materials and Methods).

Black line, the average mutual information of a 2-cell channel (1.01 bits); red line, the average mutual information of a single-cell channel (0.74 bits). (**D**) Mutual information of a multiple-cell channel according to the number of cells included as single-cell channels. Blue line, the average mutual information of a multiple-cell channel composed of different cells, $I_{\mathrm{d}}(R;S)$. Bar indicates standard deviation. Blue line ends at 2^5 cells because the sample size (the number of single-fiber) is 50. Red lines, the mutual information of a multiple-cell channel composed of 50 copies of the same cell by resampling responses repetitively from the same cell, $I_{\mathrm{s}}(R;S)$. Black line, the average $I_{\mathrm{s}}(R;S)$. Bar indicates standard deviation. Green line, mutual information of an extrapolated multiple-cell channel comprised of different cells generated by extrapolating the standard deviation to the number of cells (Eq. 11 in Materials and Methods). (**E**) The contribution of $\Delta H(R)$ and $-\Delta H(R|S)$ to $\Delta I_{\mathrm{d}}(R;S)$ in a multiple-cell channel composed of different single-cell channels. (Eqs. 16, 17 and 18 in Materials and Methods). (**F**) The contribution of $\Delta H(R)$ and $-\Delta H(R|S)$ to $\Delta I_{\mathrm{s}}(R;S)$ in a multiple-cell channel composed of copies of the same single-cell channel. I used the optimal input probability distribution for the summed response of the total cells to calculate the mutual information and the optimal input probability distribution for each channel to calculate channel capacity (dashed lines in B).

3.6 Information transmission of human facial muscle contraction

I next examined information transmission of muscle contraction *in vivo*. Human facial muscle contractions by electromyography in response to 10 repetitive EPS of facial nerves at 20 different currents in five human patients were measured during intraoperative neurophysiological monitoring (Fig. 15A, 16A) by the collaboration with Tokyo University Hospital (see Acknowledgements). I calculated the peak-to-peak amplitude of the electromyogram (Fig. 16B), a measure of muscle contraction (*34*, *35*) (Fig. 15B-D, 17). I calculated the mutual information between EPS and contraction (Fig. 15B-D). I used the optimal input probability distribution to each muscle contraction to calculate maximum mutual information, *i.e*. channel capacity. The channel capacities of facial muscle contraction were similar, between around 2 to 3 bits for each muscle (Fig. 15, 17). Because this is more information than I determined were transmitted for the Ca^{2+} response in single C2C12 myotubes (1.45 bits) and for contraction of single-fiber cells (1.38 bits) (Fig. 6E, 14B), mutual information for facial muscle contraction appeared best determined from a multiple-cell channel.

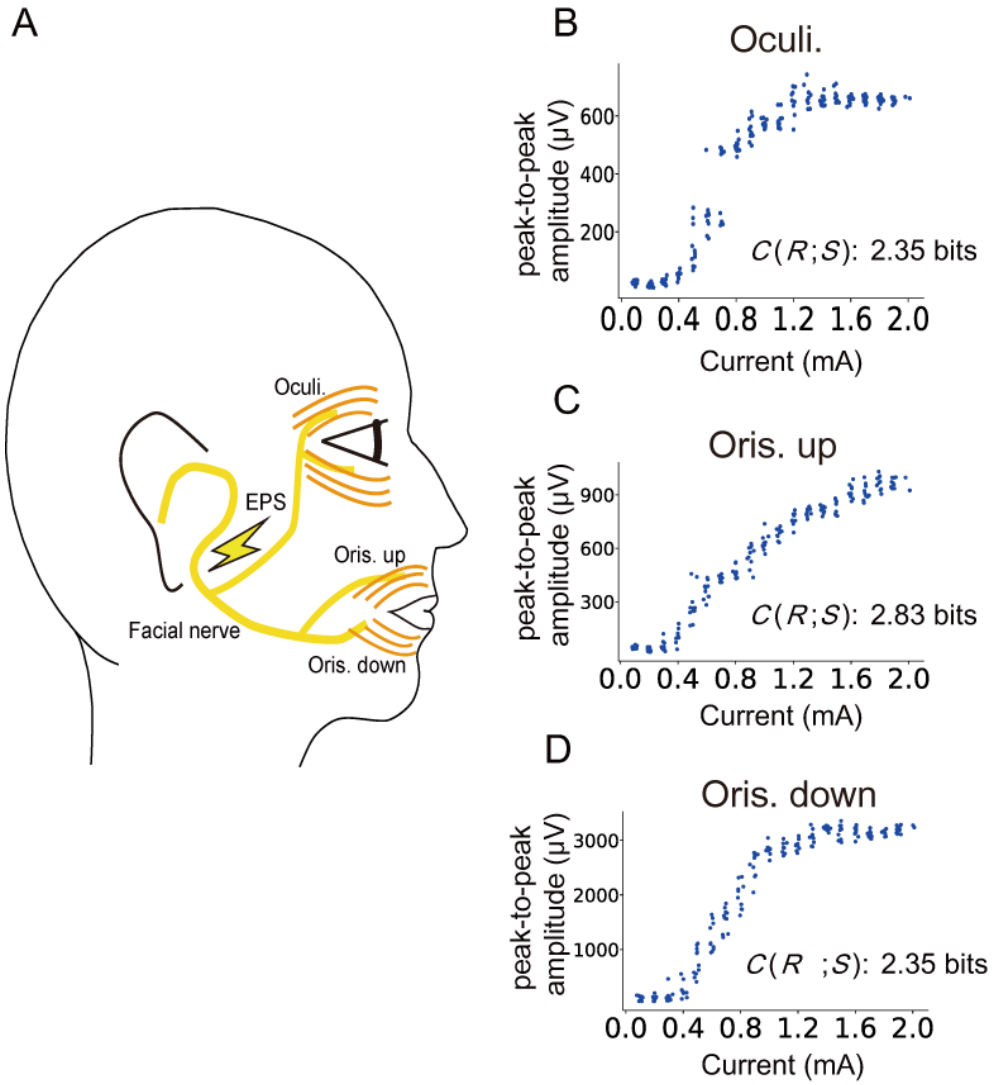

Fig. 15 Information transmission of human facial muscle contraction. (**A**) Diagram of intraoperative continuous monitoring of evoked facial nerve electromyograms in patients undergoing acoustic neuroma surgery. EPS is electrical pulse stimulation, Oculi. is orbiculis oculi muscle, and Oris. oribiculis oris muscle. (**B-D**) Dose-response of human facial muscle contraction by EPS in the orbiculis oculi muscle and up and down orbiculis oris muscles. The channel capacity in each muscle is shown. A dot indicates peak-to-peak amplitude to each single stimulation. Peak-to-peak amplitude is defined as the maximum response of the electromyogram subtracted by the minimum response (Fig. 16B). The results of other four patients are shown in Fig. 17.

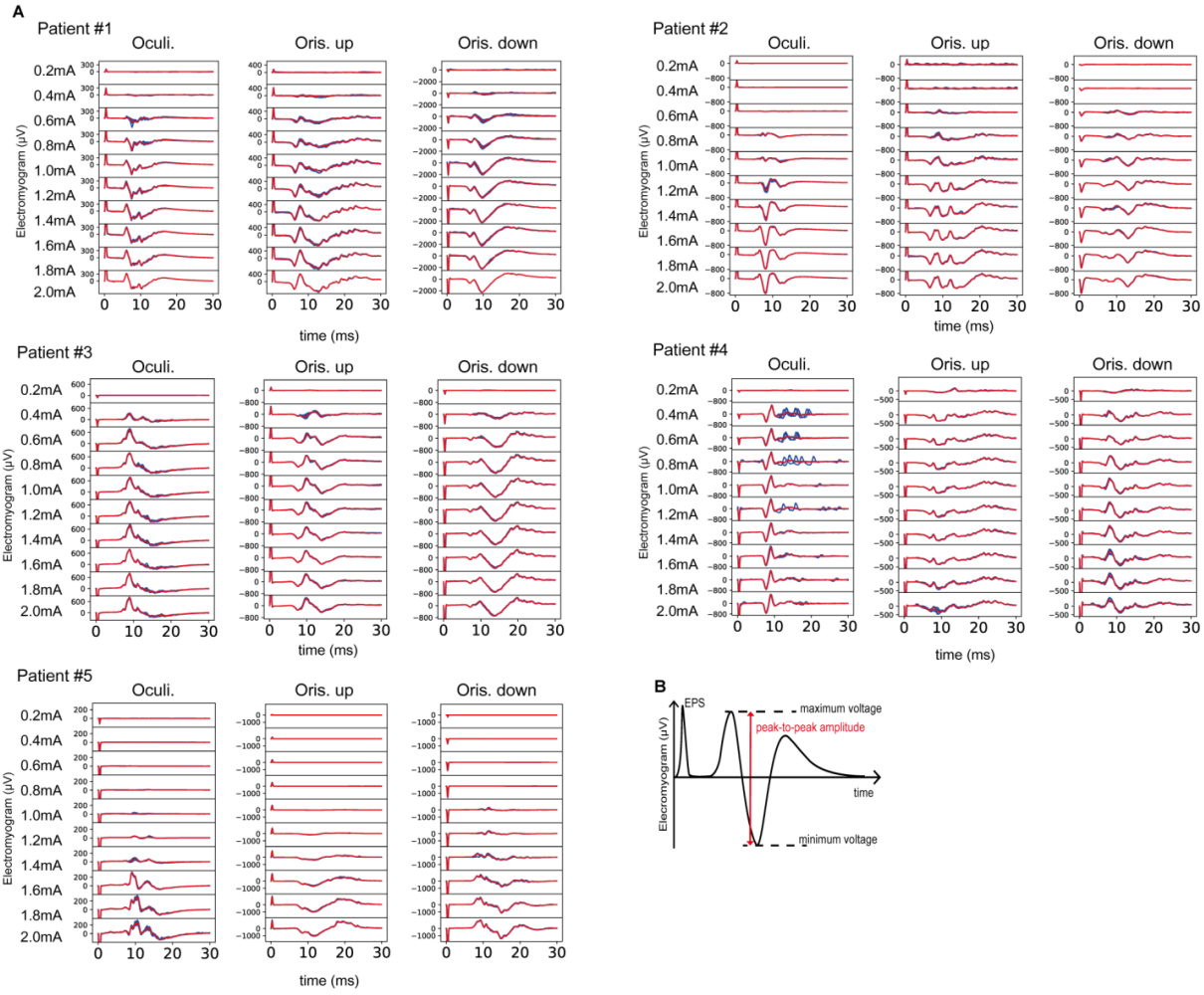

Fig. 16. Contraction of human facial muscles. (**A**) Contraction of human facial muscles (Oculi, Oris. up, Oris. down) in response to 10 times-repetitive stimulation with 20 different currents of EPS from 0.1 - 2.0 mA in patient #1 (Fig. 15), #2 (Fig. 17A), #3 (Fig. 17B), #4 (Fig. 17C), and #5 (Fig. 17D). Each blue line indicates a time course of the contraction by a single stimulation for each cell. Red lines indicate the averaged time course. (**B**) Peak-to-peak amplitude is defined as the maximum response of the electromyogram subtracted by the minimum response.

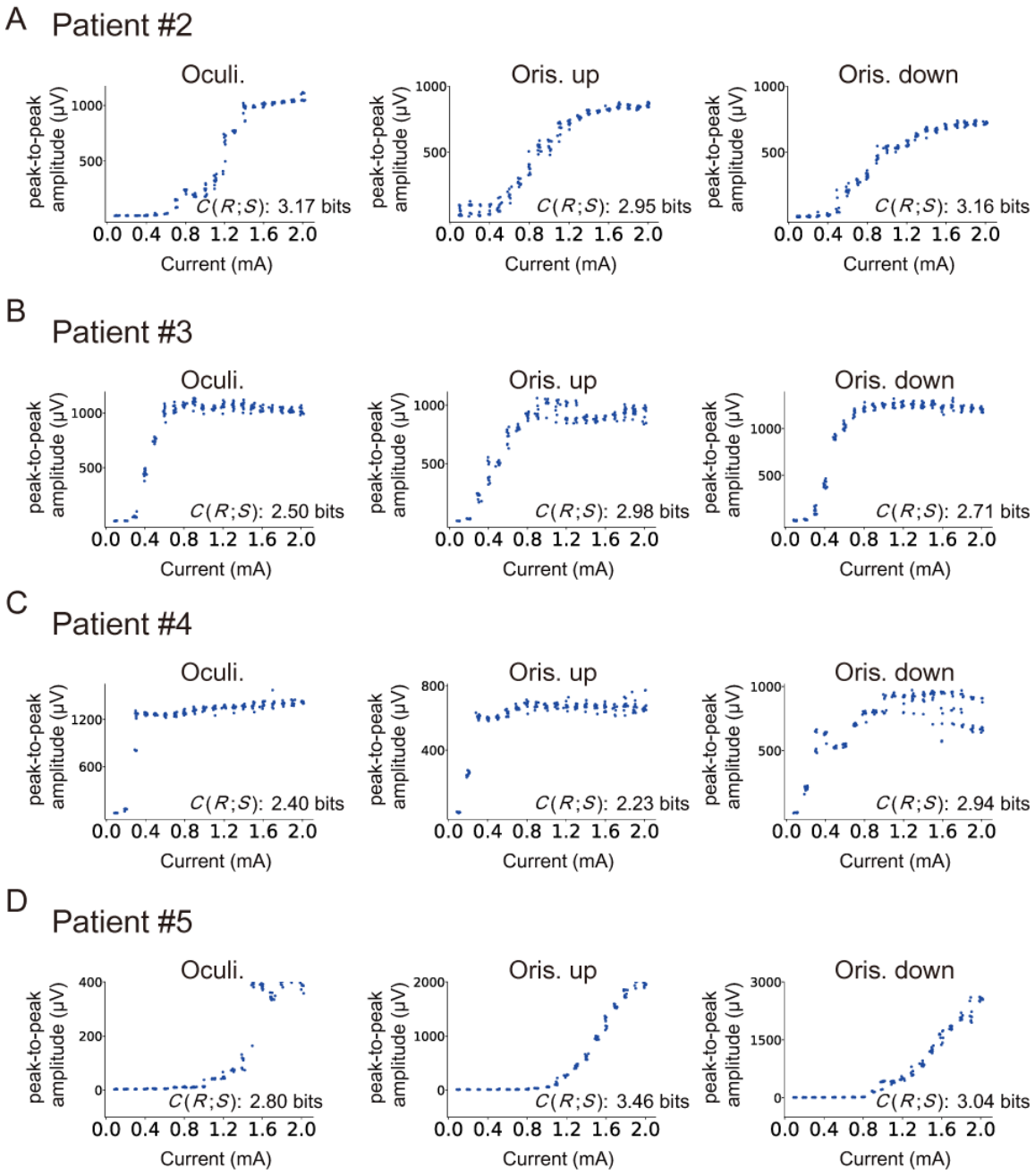

Fig. 17. Information capacity of human facial muscle contraction in the patients #2 and #3. Dose-response curves for human facial muscle contraction in patients #2 (**A**),#3 (**B**), #4 (**C**) and #5 (**D**). The channel capacity in each muscle is shown.

All skeletal muscle fibers in a muscle do not receive the same stimulation. A muscle is innervated and controlled by multiple motor neurons. A set of a motor neuron and innervated skeletal muscle fibers is known as a motor unit (Fig. 18A) (*36*). Motor neuron activity varies according to activation threshold, resulting in contraction of a skeletal muscle by summing the contraction of skeletal muscle fibers in each motor unit, a process known as recruitment (*24*). As the stimulation becomes stronger, the more motor units are recruited and muscle contraction becomes stronger. Thus, the mutual information between EPS and muscle contraction involves not only the effect of skeletal muscle fiber contraction but also that of recruited motor neurons. Therefore, it remains unclear whether the intercellular variation of skeletal muscle fibers could contribute to the increase in the mutual information of a skeletal muscle even in the presence of the effect of recruitment of motor neurons.

3.7 Intercellular variation can contribute to increase in information transmission even in the presence of the effect of motor neurons

To address this issue, I constructed a mathematical model of three serial channels considering the recruitment of motor units (Fig. 18A). In this model, S denotes EPS, N denotes the response of motor neurons, M denotes the contraction of muscle fibers, and R denotes the summed muscle contraction. In the channel from S to N, N remains zero below a threshold of S, θ, and monotonically increases above θ (Fig. 18B, 19). In the channel from N to M, I constructed the channels with or without intercellular variation, and examined the contribution of the intercellular variation of skeletal muscle fibers (Fig. 18C, D). In the

channel with intercellular variation, responses were resampled from different cells (Fig. 18C). In the channel without intercellular variation, responses were resampled from the same cell (Fig. 18D). In the channel from *M* to *R*, muscle contraction *R* is the sum of *M*, the sum of all muscle fibers. I calculated mutual information between EPS *S* and muscle contraction *R*. Mutual information with intercellular variation, $I_{\mathrm{d}}(R;S)$ (Fig. 18E, blue), was larger than most of mutual information without intercellular variation, $I_{\mathrm{s}}(R;S)$ (Fig. 18E, red), indicating that intercellular variation of muscle fiber contraction can contribute to information transmission of muscle contraction, even in the presence of the effect of recruited motor neurons.

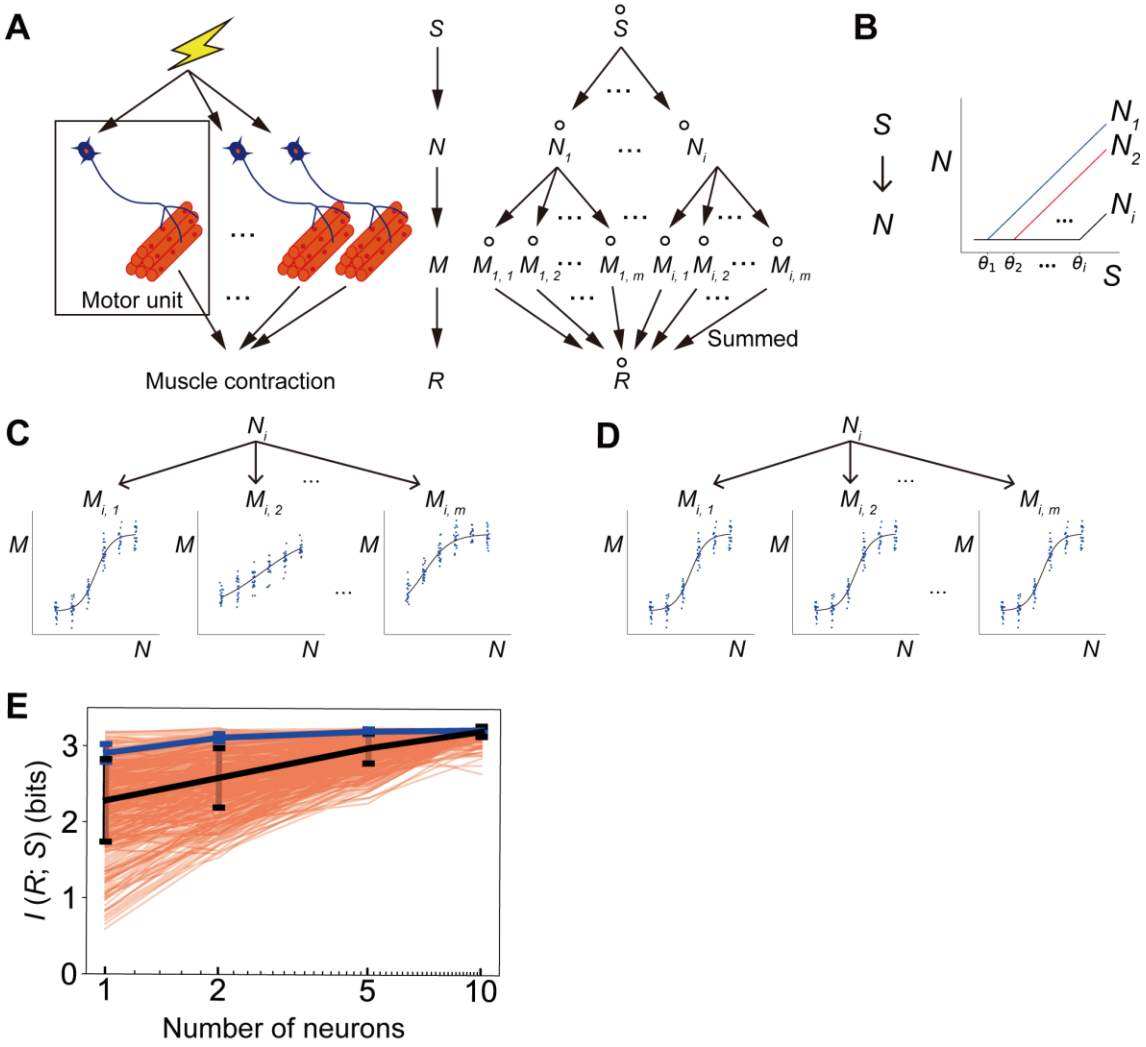
A
S
N
M
R
Motor unit
Muscle contraction
Summed
B
S
N
θ1 θ2 ... θi
S
C
M
N
D
E
I (R; S) (bits)
Number of neurons

Fig. 18 The mathematical model of muscle contraction including motor neurons.

(**A**) EPS-dependent muscle contraction through motor neurons (left). Three serial channels from stimulus *S* to neuron *N*, from neuron *N* to motor unit *M*, and from motor unit *M* to response *R* (right). (**B**) The channel from *S* to *N*. The response of motor neurons with the different thresholds, θ. Note that each neuron has a different threshold. Because experimentally I used 10 steps of stimulation intensity, I set the numbers of thresholds as divisors of 10: 1, 2, 5, and 10 (Fig. 19). (**C**, **D**) The channel from *N* to *M* with intercellular variation (C) and without intercellular variation (D). The dose -responses of muscle fibers are controlled by the neurons with a certain threshold. I used Ca^{2+} response in C2C12 myotubes as muscle fiber response, and the responses were resampled from different cells (C) or from the same cell (D). I set 64 muscle fibers controlled by each neuron with the same threshold (Fig. 21). (**E**) The mutual information with intercellular variation, $I_{\mathrm{d}}(R;S)$ (blue), and without intercellular variation, $I_{\mathrm{s}}(R;S)$ (red), and the average of $I_{\mathrm{s}}(R;S)$ (black). Bars indicate standard deviation for both black and blue lines.

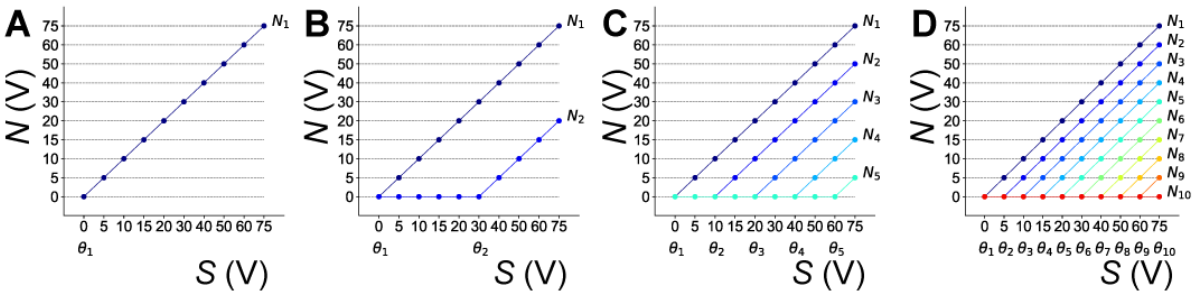

Fig. 19. The channel from *S* to *N* with different numbers of neurons. (**A**–**D**) The numbers of neurons are 1 (A), 2 (B), 5 (C), and 10 (D). I used 10 voltages for stimulation intensity *S*; 0, 5, 10, 15, 20, 30, 40, 50, 60, and 75 V (Fig. 6). I modeled *N* as a nonlinear transformation of *S* on a discrete space composed of the 10 voltages according to the corresponding threshold. I set the number of thresholds as divisors of 10: 1, 2, 5, and 10. *N* is an effective voltage given to *M*. When the number of neurons is 1 (A), θ_1 is 0 V and *N* monotonically increases, meaning that *N* is equal to *S*. When the number of neurons is 2 (B), θ_1 is 0 V and θ_2 is at 30 V. This means that for N_2, N_2 is 5 V when *S* is 40 V, N_2 is 10 V when *S* is 50 V, *etc*. I set θ as 0, 10, 20, 40, and 60 V for five thresholds (C), and as 0, 5, 10, 15, 20, 30, 40, 50, 60, and 75 V for ten thresholds (D). Note that interval of voltages in the *x*- and *y*-axes are not equal.

In this model, I did not include noise in the channel from *S* to *N*. However, there must be noise and response of neurons fluctuates. Therefore, the contribution of neurons is overestimated and the contribution of intercellular variation is underestimated in our calculations. The reduction in the difference between $I_{\mathrm{d}}(R;S)$ and $I_{\mathrm{s}}(R;S)$ that occurred with the increase in the number of neurons was an artifact caused by the number of steps of stimulation intensity used in the experiments (Fig. 20). The difference between $I_{\mathrm{d}}(R;S)$ and $I_{\mathrm{s}}(R;S)$ should remain regardless of the number of neurons.

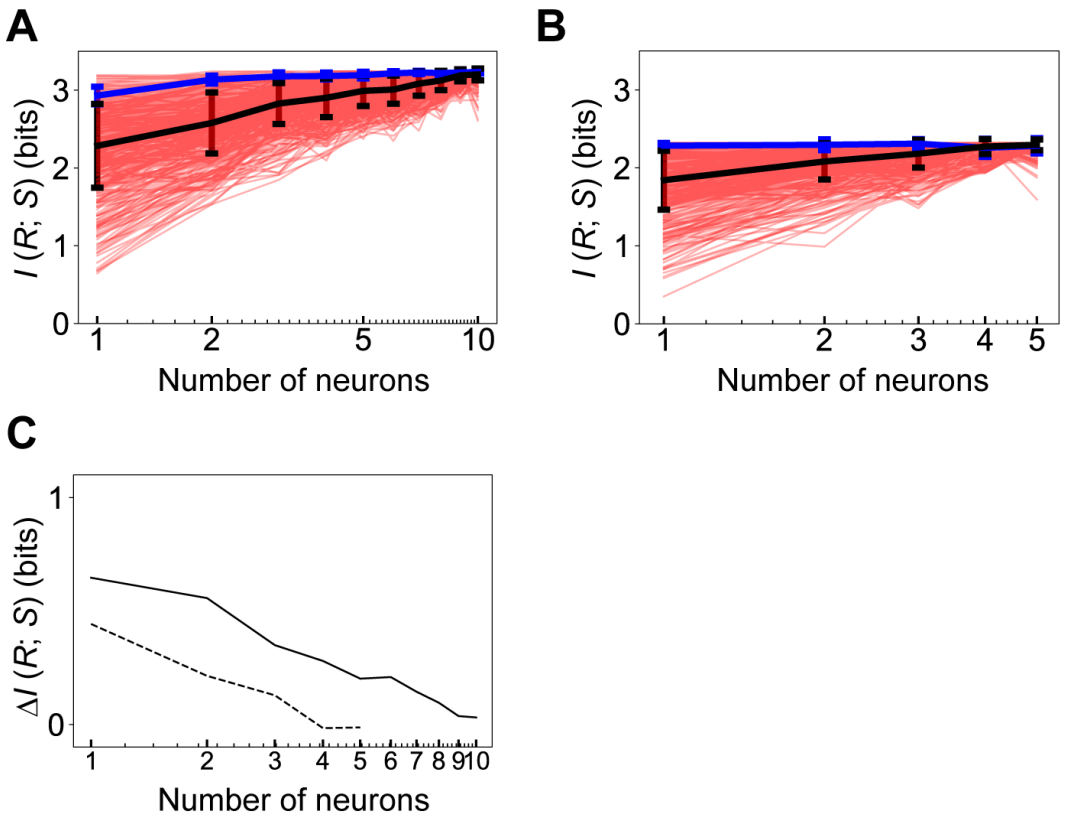

Fig. 20. The effect of the number of steps of stimulation intensity on mutual information with or without intercellular variation. (**A-B**) The mutual information with intercellular variation, $I_{\mathrm{d}}(R;S)$ (blue), and without intercellular variation, $I_{\mathrm{s}}(R;S)$ (red), and the average of $I_{\mathrm{s}}(R;S)$ (black) when the number of steps of stimulation intensity is 10 (A) and 5 (B). (**C**) The difference between $I_{\mathrm{d}}(R;S)$ and $I_{\mathrm{s}}(R;S)$, $\Delta I(R;S)$, when the number of steps of stimulation intensity is 10 (solid) and 5 (dashed). When the number of steps of stimulation intensity is 10, $\Delta I(R;S)$ becomes close to 0 when the number of neurons is 10. When the number of steps of stimulation intensity is 5, $\Delta I(R;S)$ becomes close to 0 when the number of neurons is 5. In both cases, $\Delta I(R;S)$ becomes close to 0 at the number of neurons reaches the number of steps of stimulation intensity. The reduction in the difference between $I_{\mathrm{d}}(R;S)$ and $I_{\mathrm{s}}(R;S)$ according to the increase in the number of neurons is an artifact caused by the number of steps of stimulation intensity.

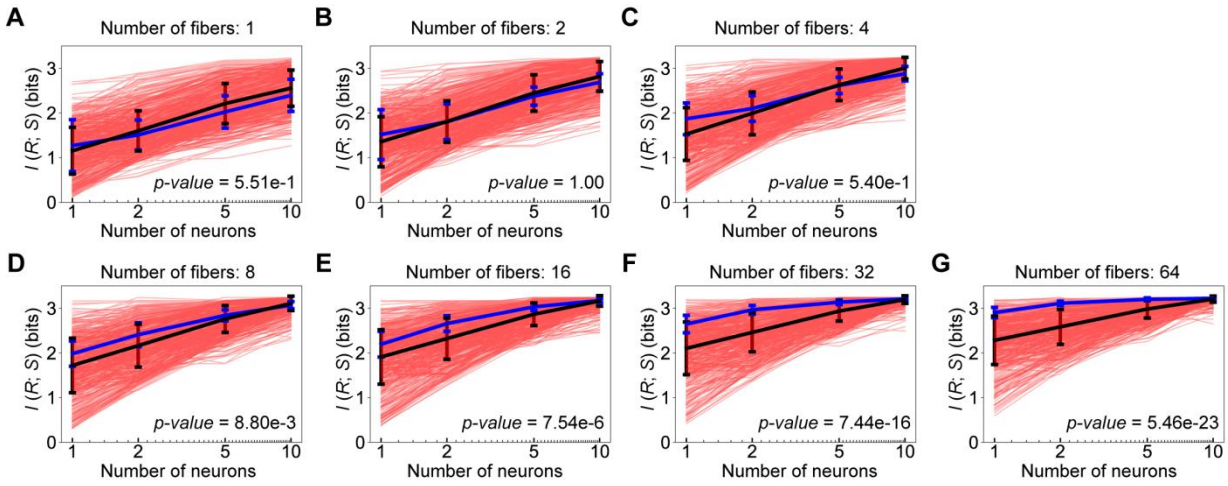

Fig. 21. $I_{\mathrm{d}}(R;S)$ and $I_{\mathrm{s}}(R;S)$ with different numbers of muscle fibers controlled by each neuron. (**A-G**) The mutual information is plotted with intercellular variation, $I_{\mathrm{d}}(R;S)$ (blue), and without intercellular variation, $I_{\mathrm{s}}(R;S)$ (red), and the average of $I_{\mathrm{s}}(R;S)$ (black) with indicated number of muscle fibers controlled by each set of neurons. I performed a two-way ANOVA with number of neurons and group (with/without intercellular variation) as the independent variables, and mutual information as the dependent variable (see Methods) for each number of muscle fibers controlled by each neuron. The Bonferroni adjusted *p*-values (n = 7; the number of panels) between mutual information and group are shown in each panel. The mutual information with or without intercellular variation is significantly different when a number of muscle fibers controlled by each neuron is more than 4, indicating that the intercellular variation can contribute to increase in information capacity even when a small number of muscle fibers are controlled by neurons. Therefore, it is physiologically plausible that intercellular variation can contribute to increase in information capacity.

4. Discussion

4.1 Biological meaning of the output of multiple-cell channels

In this study, I examined the information transmission of a muscle composed of multiple muscle fibers for which the output (contraction) is the sum of responses of individual cells. Another biological example is the regulation of hormone secretion, for which the total amount of a hormone released is the sum of the hormone secreted from individual cells. The analysis in this study indicated that, like muscle contraction, secretion of a hormone can be regulated more precisely in the presence of intercellular variation than in the absence. When single-cell response is switch-like, both intracellular variation and intercellular variation can contribute to information transmission capacity of the multiple-cell channel by stochastic resonance (*37*). The results showed that the intercellular variation can increase information capacity through the response diversity effect even when single-cell response is not switch-like.

4.2 Gradualness of the dose-response of cell-population

I found that intercellular variation can serve as information rather than noise. Intercellular variation increased information transmission through a response diversity effect: The dose-response of a multiple-cell channel becomes more gradual than that of a single-cell channel, resulting in increase in information entropy, $H(R)$. A similar gradualness of the response at a cell-population level occurs in progesterone-induced mitogen-activated protein kinase (MAPK) activation in *Xenopus* oocytes (*38*). MAPK activation in individual cells

shows all-or-none responses, and the thresholds for MAPK activation differ between individual cells. Therefore, the dose-response relationship for MAPK activation at the cell-population level becomes gradual. If the amount of secreted progesterone gradually changes in response to environmental and nutrient conditions, the number of mature oocytes can be gradually controlled. The response diversity effect may also contribute to the precise regulation of the number of mature oocytes in response to changes in environmental and nutrient conditions. Because the experiments with MAPK activation were "snapshot" experiments (Fig. 1D), those data cannot differentiate whether the different responses between individual cells is derived from intercellular variation or from intracellular variation. Dueck *et al*. proposed a hypothesis that graded population response mediated by individual variation can be functionally important mechanism bridging the discrete outputs of a cell and quantitative response in their essay (*39*), which is similar to the idea of response diversity effect. However, it is not explicitly mentioned whether the individual variation is derived from intercellular variation or from intracellular variation.

4.3 Multiple-cell channel with intercellular variation

Some previous studies evaluated the effect of the cell-population size on the mutual information of multiple-cells. However, intercellular and intracellular variations were not distinguished in those works because they did not stimulate the cells repetitively. Cheong *et al*. (*14*) showed that the mutual information of a multiple-cell channel increases as the number of cells increases, though response diversity effect and large number effect were not

distinguished. Sudarman *et al*. (*21*) showed that variation in the single-cell response can increase mutual information of the response of multiple-cells; however, the increase in mutual information in their work was due to stochastic resonance.

Thus, the contribution of intercellular variation to the gradual dose-response and to the increase in mutual information by large sample size did not be investigated. Ferrell *et al*. showed a that a cell-population level analysis could produce a gradual dose-response relationship (*38*), whereas Cheong *et al*. (*14*) and Sudarman *et al*. (*21*) showed that information transmission in multiple-cell channels is greater than that of single-cell channels. Here, I integrated these two concepts— gradual dose-response at cell-population level and an increase of information transmission in multiple-cells— into the concept of the response diversity effect, which explained how intercellular variation can increase information transmission.

4.4 Summaty and conclusion

In skeletal muscle cells, I found that intracellular variation is small and intercellular variation is large, which means that each cell responds accurately and reproducibly to a particular stimulus, but their responses differ from each other. Under such conditions, intercellular variation can have a large contribution to information transmission capacity. Intercellular variation can be derived from the differences in gene expression and protein abundance among cells (*2, 3*), as well as metabolic differences. I anticipate that many biological systems use a combination of intracellular and intercellular variation, in different

ways, to precisely control responses to a range of stimuli. Thus, multiple-cell channels provide the best representation for determining information capacity of biological tissues and organs. The ability to calculate and model information capacity will enable researchers to explore tissue-level responses, understand how biological variation of cells of the same type contribute to the dynamic range of stimulus-response profiles, and investigate how cellular dysfunction that alters intercellular variation can contribute to disease, such as occurs in muscular dystrophy or diseases associated with impaired muscle contraction.

5. References

1. B. Alberts et al., Molecular Biology of the Cell (Garland Science, New York, ed. 5, 2008).

2. M. B. Elowitz, A. J. Levine, E. D. Siggia, P. S. Swain, Stochastic gene expression in a single cell. *Science* **297,** 1183-1186 (2002).

3. P. S. Swain, M. B. Elowitz, E. D. Siggia, Intrinsic and extrinsic contributions to stochasticity in gene expression. *Proc. Natl. Acad. Sci. U.S.A.* **99,** 12795–12800 (2002).

4. C. E. Shannon, A Mathematical Theory of Communication. *Bell Syst. Tech. J.* **27**, 379–423 (1948).

5. C. E. Shannon, A Mathematical Theory of Communication. *Bell Syst. Tech. J.* **27**, 623–656 (1948).

6. P. J. Thomas, D. J. Spencer, S. K. Hampton, P. Park, J. P. Zurkus, paper presented at Neural Information Processing Systems, NIPS2003, Vancouver, British Columbia, Canada, 8 to 13 December 2003.

7. G. Tkačik, C. G. Callan Jr., W. Bialek, Information flow and optimization in transcriptional regulation. *Proc. Natl. Acad. Sci. U.S.A.* **105,** 12265–12270 (2008).

8. G. Tkačik, C. G. Callan Jr., W. Bialek, Information capacity of genetic regulatory elements. *Phys. Rev. E Stat. Nonlin. Soft Matter Phys.* **78,** 011910 (2008).

9. R. C. Yu, C. G. Pesce, A. Colman-Lerner, L. Lok, D. Pincus, E. Serra, M. Holl, K. Benjamin, A. Gordon, R. Brent, Negative feedback that improves information transmission in yeast signalling. *Nature* **456,** 755–761 (2008).

10. T. Lenaerts, J. Ferkinghoff-Borg, J. Schymkowitz, F. Rousseau, Information theoretical quantification of cooperativity in signalling complexes. *BMC Syst. Biol.* **3,** 9 (2009).

11. P. Mehta, S. Goyal, T. Long, B. L. Bassler, N. S. Wingreen, Information processing and signal integration in bacterial quorum sensing. *Mol. Syst. Biol.* **5,** 325 (2009).

12. I. Lestas, G. Vinnicombe, J. Paulsson, Fundamental limits on the suppression of molecular fluctuations. *Nature* **467,** 174–178 (2010).

13. Tostevin, P. R. ten Wolde, Mutual information in time-varying biochemical systems. *Phys. Rev. E Stat. Nonlin. Soft Matter Phys.* **81,** 061917 (2010).

14. R. Cheong, A. Rhee, C. J. Wang, I. Nemenman, A. Levchenko, Information transduction capacity of noisy biochemical signaling networks. *Science* **334,** 354–358 (2011).

15. C. Waltermann, E. Klipp, Information theory based approaches to cellular signaling. *Biochim. Biophys. Acta* **1810,** 924–932 (2011).

16. S. Uda, T. H. Saito, T. Kudo, T. Kokaji, T. Tsuchiya, H. Kubota, Y. Komori, Y. Ozaki, S. Kuroda, Robustness and compensation of information transmission of signaling pathways. *Science* **341,** 558–561 (2013).

17. M. Voliotis, R. M. Perrett, C. McWilliams, C. A. McArdle, C. G. Bowsher, Information transfer by leaky, heterogeneous, protein kinase signaling systems. *Proc. Natl. Acad. Sci. U.S.A.* **111**, E326–E333 (2014).

18. J. Selimkhanov, B. Taylor, J. Yao, A. Pilko, J. Albeck, A. Hoffmann, L. Tsimring, R. Wollman, Accurate information transmission through dynamic biochemical signaling networks. *Science* **346,** 1370–1373 (2014).

19. K. L. Garner, R. M. Perrett, M. Voliotis, C. Bowsher, G. R. Pope, T. Pham, C. J. Caunt, K. Tsaneva-Atanasova, C. A. McArdle, Information transfer in gonadotropin-releasing hormone (GnRH) signaling: extracelluar signal-regulated kinase (ERK)-mediated feedback loops control hormone sensing. *J. Biol. Chem.* **291,** 2246-2259 (2016).

20. G. D. Potter, T. A. Byrd, A. Mugler, B. Sun, Dynamic sampling and information encoding in biochemical networks. *Biophys. J.* **112,** 795-804 (2017).

21. R. Suderman, J. A. Bachman, A. Smith, P. K. Sorger, E. J. Deeds, Fundamental trade-offs between information flow in single cells and cellular populations. *Proc. Natl. Acad. Sci. U.S.A.* **114,** 5755-5760 (2017).

22. A. A. Granados, J. M. J. Pietsch, S. A. Cepeda-Humerez, I. L. Farquhar, G. Tkacik, P. S. Swain, Distributed and dynamic intracellular organization of extracellular information. *Proc. Natl. Acad. Sci. U.S.A.* **115,** 6088-6093 (2018).

23. A. Keshelava, G. P. Solis, M. Hersch, A. Koval, M. Kryuchkov, S. Bergmann, V. L. Katanaev, High capacity in G protein-coupled receptor signaling. *Nat Commun.* **9,** 876 (2018).

24. R. E. Burke, D. N. Levine, F. E. Zajac, P. Tsairis, W. K. Engel, Mammalian motor units: physiological-histochemical correlation in three types in cat gastrocnemius. *Science*. **174**, 709–12 (1971).

25. T. W. Chen, T. J. Wardill, Y. Sun, S. R. Pulver, S. L. Renninger, A. Baohan, E. R. Schreiter, R. A. Kerr, M. B. Orger, V. Jayaraman, L. L. Looger, K. Svoboda, D. S. Kim, Ultrasensitive fluorescent proteins for imaging neuronal activity. *Nature* **499,** 295–300 (2013).

26. K. Yusa, R. Rad, J. Takeda, A. Bradley, Generation of transgene-free induced pluripotent mouse stem cells by the piggyBac transposon, *Nat. Methods*, **6,** 5363–369 (2009).

27. S. J. Odelberg, A. Kollhoff, M. T. Keating, Dedifferentiation of mammalian myotubes induced by msx1. *Cell,* **103**(7), 1099–1109 (2000).

28. G. Shefer, Z. Yablonka-Reuven, Isolation and culture of skeletal muscle myofibers as a means to analyze satellite cells. *Methods Mol. Biol*. **290,** 281-304 (2005).

29. Y. Manabe, S. Miyatake, M. Takagi, M. Nakamura, A. Okeda, T. Nakano, M. F. Hirshman, L. J. Goodyear, N. L. Fujii, Characterization of an acute muscle contraction model using cultured C2C12 myotubes. *PLoS ONE* **7**(12): e52592 (2012).

30. Y. Manabe, S. Ogino, M. Ito, Y. Furuichi, M. Takagi, M. Yamada, N. Goto-Inoue, Y. Ono, N. L.Fujii. Evaluation of an in vitro muscle contraction model in mouse primary cultured myotubes. *Anal Biochem.* **497,** 36-38 (2016).

31. G. A. Darbellay, I. Vajda, Estimation of the information by an adaptive partitioning of the observation space. *IEEE Trans. Inf. Theory* **45,** 1315–1321 (1999).

32. S. Arimoto, An algorithm for computing the cap*acity of arbitrary disc*rete memoryless channels. *IEEE Trans. Inf. Theory* **18,** 14–20 (1972).

33. R. E. Blahut, Computation of channel capacity and rate-distortion functions. *IEEE Trans. Inf. Theory* **18,** 460–473 (1972).

34. H. Nakatomi, H. Miyazaki, M. Tanaka, , T. Kin, M. Yoshino, H. Oyama, M. Usui, H. Moriyama, H. Kojima, K. Kaga, N. Saito. Improved preservation of function during acoustic neuroma surgery. *J. Neurosurg*., **122**, 24-33 (2015).

35. M. Amano, M. Kohno, O. Nagata, M. Taniguchi, S. Sora, H. Sato, Intraoperative continuous monitoring of evoked facial nerve electromyograms in acoustic neuroma surgery. *Acta Neurochir.* **153**, 1059–1067 (2011).

36. C. J. Heckman, R. M. Enoka, Motor unit, *Compr. Physiol.*, **2,** 2629–2682 (2012).

37. L. Gammaitoni, P. Hänggi, P. Jung, F. Marchesoni, Stochastic resonance. *Rev. Mod. Phys.* **70**, 223–287 (1998).

38. J. E. Ferrell, E. M. Machleder, The Biochemical basis of an all-or-none cell fate switch in Xenopus oocytes. *Science.* **280**, 895–898 (1998).

39. H. Dueck, J. Eberwine, J. Kim, Variation is function: Are single cell differences functionally important? *BioEssays*. **38**, 172–180 (2016).

6. Acknowledgments

I thank my laboratory members for critically reading this manuscript and for their technical assistance with the experiments. Especially, I would like to express my greatest appreciation to Professor Shinya Kuroda for teaching principles of scientific research throughout my graduate study. This thesis is the result of the joint research of Mr. Mitustaka Wataya, Dr. Miki Eto, Dr. Daisuke Hoshino, Dr. Katsuyuki Kunida and me in the experiments of differentiated C2C12 myotubes, and Dr. Haruki Inoue, Mr. Mitustaka Wataya, Dr. Masashi Fujii and me in image analysis, Dr. ken-ichi Hironaka, Mr. Mitustaka Wataya, Dr. Masashi Fujii, Dr. Shinsuke Uda, Dr. Hiroyuki Kubota and me in computational analysis, Mr. Hiroki Hamaguchi, Dr. Yasuro Furuichi, Dr. Yasuko Manabe, and Dr. Nobuharu L. Fujii in Tokyo Metropolitan University in the experiments of isolated skeletal muscle fibers, Dr. Tsuguto Takizawa, Dr. Yasuaki Karasawa, Dr. Hirofumi.Nakatomi, and Dr. Nobuhito Saito in Tokyo University Hospital in intraoperative neurophysiological monitoring. This manuscript was edited by Nancy R. Gough (BioSerendipity, LLC).

This work was supported by the Creation of Fundamental Technologies for Understanding and Control of Biosystem Dynamics, CREST (JPMJCR12W3) from the Japan Science and Technology Agency (JST) and by the Japan Society for the Promotion of Science (JSPS) KAKENHI Grant Number (JP17H06299, JP17H06300, JP18H03979, JP19K22860).